DESIGN OF FREQUENCY DEPENDENT IMPEDANCE

FOR TRANSMISSION LINE MODELING

by

William Edward Feero

Bachelor of Science, University of Maine
1960

Master of Science, University of Pittsburgh
1969

SUBMITTED IN PARTIAL FULFILLMENT OF THE

REQUIREMENTS FOR THE DEGREE OF

ELECTRICAL ENGINEER

at

MASSACHUSETTS INSTITUTE OF TECHNOLOGY

September 1971 (i.e. Feb. 1972)

Signature of Author Signature redacted
Department of Electrical Engineering, September 29, 1971

Certified by Signature redacted
Thesis Supervisor

Accepted by Signature redacted
Chairman, Departmental Committee on Graduate Students

DESIGN OF FREQUENCY DEPENDENT IMPEDANCE FOR TRANSMISSION LINE MODELING

by

William Edward Feero

Submitted to the Department of Electrical Engineering on September 29, 1971 in partial fulfillment of the requirements for the degree of Electrical Engineer.

ABSTRACT

This thesis develops a technique for simulating frequency dependent resistance and inductance. The frequency dependence is designed to match that of the earth return path of a three phase power transmission line. It is intended for use in the TLM, transmission line model, of the TSS, transmission system simulator, which will primarily be used by the Electric Power Systems Engineering Laboratory. The TSS will be normally used to conduct switching surge studies.

A comprehensive review of work by early researchers in the area of frequency response characteristics of transmission lines is presented. From this work it is shown how to develop the actual resistance and inductance characteristics required for the TLM earth return parameters. The analysis presented considers frequencies from .1 to 5000 Hz and earth resistivities between 10 to 1000 Ohm-meters.

To develop a resistance and inductance that would have the same frequency response found for the actual transmission line, a long solid metallic rod was wrapped with wire to create a long solenoid inductor. A detailed diffusion analysis of this configuration is presented. Various types of metals are investigated and the limitations of each discussed, in particular the ferromagnetic metals.

From experience gained during the long solenoid investigation, it was found that a frequency dependent impedance using the diffusion phenomena could be achieved by creating a "short solenoid", disks of highly conducting metal between the pole faces of two powdered iron yokes. A method for selecting the proper disk size to match a given line configuration is given. Also since a single disk circuit does not adequately represent the required transmission line parameter, a technique is developed to gain the required impedance by combining two disk circuits.

Complete design details are presented for simulating 4 and 8 mile sections of EHV line configurations. To prove the techniques, actual test data for various 345 and 765 kV line configurations are given. For most simulation tests the design technique matches the actual system characteristics within five percent for the frequency range of 20 to 5000 Hz.

THESIS SUPERVISOR: Gerald L. Wilson
TITLE: Associate Professor of Electrical Engineering

TABLE OF CONTENTS

TABLE OF CONTENTS

LIST OF FIGURES

LIST OF TABLES

ACKNOWLEDGMENTS

I wish to express my gratitude to Westinghouse Electric Corporation for providing the time and finances for one year of advanced study. I wish to thank Professor Gerald L. Wilson, my thesis supervisor, for the initial concept and direction of the project, for his constant availability and interest, and for his timely suggestions, comments, criticisms, and guidance throughout the design. The basic premise that the diffusion characteristics of metals could be used to simulate earth effects was Professor Wilson's.

CHAPTER 1

INTRODUCTION

The design of EHV and UHV systems necessitates a very detailed analysis of system overvoltages. In particular UHV systems mandate that the overvoltage "with stand" design must be reduced to a minimum if UHV is to be economically feasible.[1] In this respect it is necessary to analyze every component that can possibly affect overvoltage conditions in the system to determine the extent they control or affect surge generation and propagation.

General purpose transmission line models for transient analysis have been available for many years.[2,3,4,5,6] In most of this modeling the circuit is composed of a passive element representation in pi section or L section form as shown in Figures 1.1 and 1.2.[7] Although satisfactory correspondence between model studies and actual field tests has been achieved in the past, there are areas of sufficient mismatch to suggest an incomplete model of the transmission line. Usually field tests produce lower maximum voltages than predicted by studies on analog models. There are many factors that may explain this difference between field tests and miniature system studies. For example, the effect of corona on the surge crest,[8] the effect of nonlinear load parameters attached behind the switching point of the transmission line, nontransposed lines modeled as

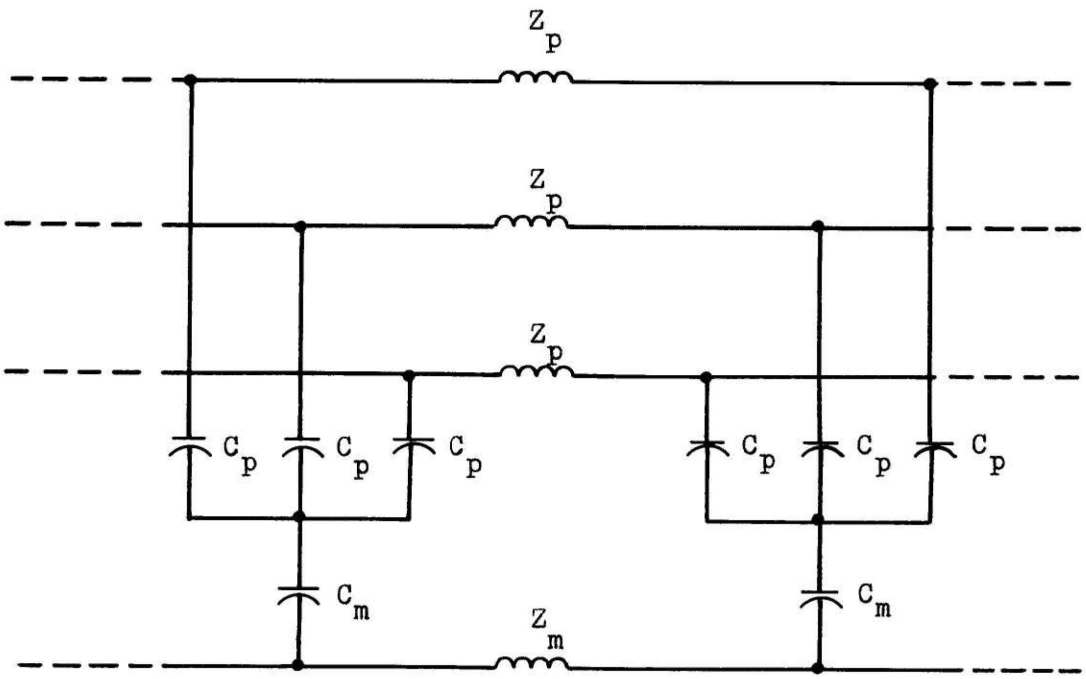

where

$Z_p = (1/N)(R_1 + j2\pi fL_1)$

$C_p = C_1/2N$

$Z_m = (1/N)((R_o-R_1)/3 + j2\pi f(L_o- L_1)/3)$

$C_m = (1/2N)((3C_1C_o)/(C_1- C_o))$

N = Number of Pi Sections in the Line

L_1, L_o, R_1, R_o, C_1, C_o are the Positive and Zero Sequence Parameters of the Total Line

Anacom Representation of Transmission Lines

Figure 1.1

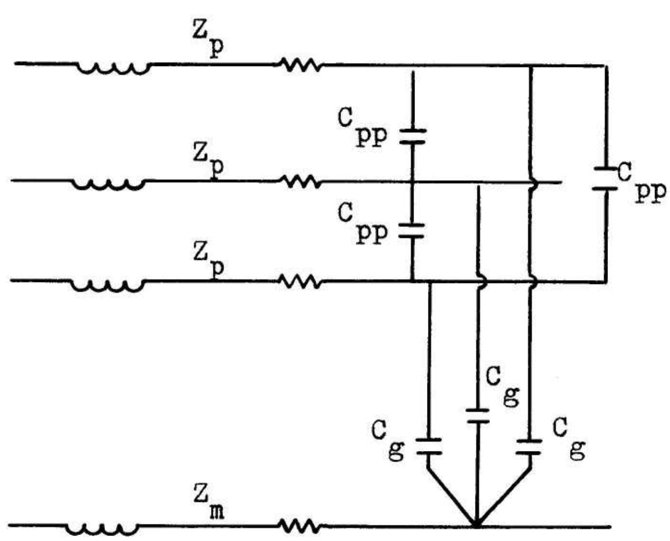

where

$Z_p = (1/N)(R_1 + j2\pi f L_1)$

$C_{pp} = (1/N)((C_1 - C_o)/3)$

$Z_m = (1/N)((R_o - R_1)/3 + j2\pi f(L_o - L_1)/3)$

$C_g = C_o/N$

N = The Number of L Sections in the Transmission Line

L_1, L_o, R_1, R_o, C_1, C_o are the Positive and Zero Sequence Parameters of the Total Line

A Three Phase L Section Representation of a Transmission Line

Figure 1.2

transposed lines,[7] and the effect of the surge propagation through the nonlinear ground path.

The effective return path impedance shown as Z_m in Figures 1.1 and 1.2 has normally been modeled with a nearly linear resistor and a linear inductor with respect to frequency. However in the 1920's and 1930's researchers had demonstrated that the effective impedance of the earth is not independent of frequency but varies as some function of frequency.[9,10] A detailed review of this work will be presented in Chapter 2 since it is fundamental to motivating the techniques presented in this thesis.

Only recently has interest developed in a more detailed and rigorous analysis where the zero sequence or earth return impedance was allowed to be a function of frequency.[11,12,13] In switching surge studies some of the initial work required an iterative analysis to find the dominant frequency.[14] Once this was found the correct impedance at this frequency was set in for Z_m. Another approach led to modeling the zero sequence characteristics by a series parallel combination of linear inductors and nonlinear resistors.[15] This approach appears to give satisfactory results but it requires six elements for the simulation.

Considerable work has been done in this area using digital computers to analyze nonlinear zero mode propagation.[13,16,17,18,19,20] However digital computers have to combine the complex mathematics of the nonlinear analysis with intricate and slow digital iterative techniques; therefore solutions can become rather expensive on generalized design studies of systems.

The analog model of a three phase section of a nontransposed transmission line as required by Mr. Schmidt's design is shown in Figure 1.3.[21] The Z_{oo} shown is similar in magnitude at 60 Hz to the Z_m's shown in Figures 1.1 and 1.2 except for an adjustment for the effect of nontransposition. Investigations have shown that at frequencies other than 60 Hz Z_{oo} differs markedly from the normal Z_m representation. For instance over the range of 5 to 5000 Hz the L_{oo} term may change by a factor of 3 to 1 and for the R_{oo} term the change is considerable greater. This thesis presents a general method for fitting both of these characteristics simultaneously over a frequency range from 20 to 5000 Hz.

Preceding work by Mr. Schmidt has established many of the constraints that are used in this analysis. The TLM, Transmission Line Model, designed by Mr. Schmidt is used to simulate the phase characteristics of a transmission line. Therefore impedance scales, number of pi sections to be used, physical size, current rating and frequency range required are all set by Mr. Schmidt's thesis. Briefly, Mr. Schmidt found the impedance scale would vary from .2 to .4 times the system

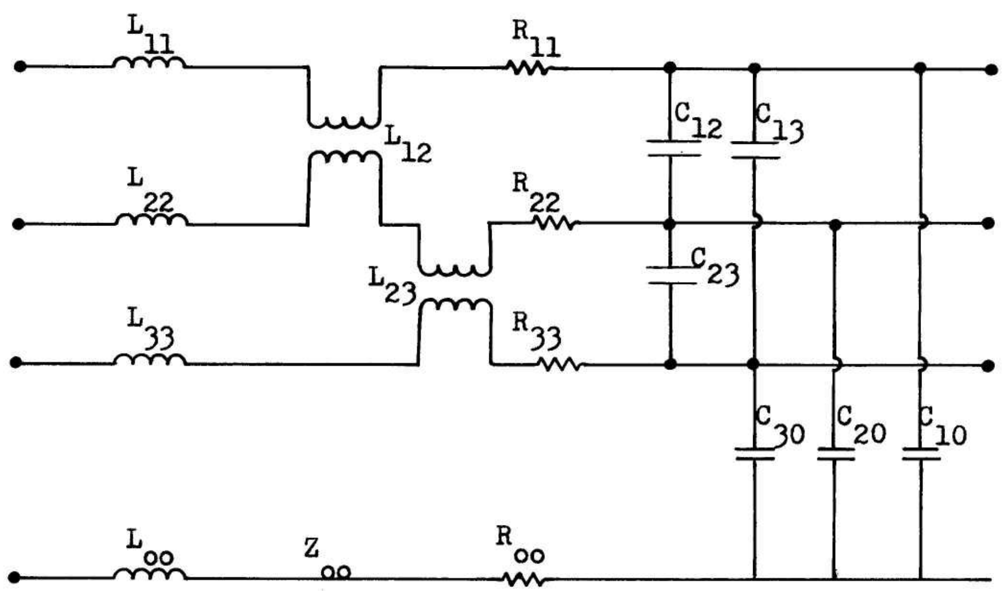

Section of a "Balance Mutual"
Non-Transposed Line Model[21]

Figure 1.3

impedance; that 4 mile and 8 mile pi sections should be built; that all the physical parameters to be used to simulate these 4 and 8 mile sections should fit in a space 11.625 x 19.0 x 9.75 inches (the arrangement of phase elements leaves a 9.0 x 9.0 x 4.0 inch volume for the earth impedance parameters;) and the frequency range for accurate modeling should be from DC through 5000 Hz. As will be demonstrated later the model built is accurate from approximately 20 Hz to 5000 Hz with the same tolerance as in Mr. Schmidt's thesis, i.e.,approximately five percent.

CHAPTER 2

CALCULATION OF EARTH EFFECTS

2.1 Carson Reviewed

To properly motivate the method used to simulate the frequency dependent earth parameters it is necessary to review the work of Carson,[9] and that of Wagner and Evans.[10] In his original work Carson did a field theory analysis of conductors in parallel with the earth using the earth as a return path. This circuit is depicted in Figure 2.1. For the purpose of this thesis consider the "a" conductor as a composite conductor representing the phase conductors of a transmission line. Similarly the "g" conductor represents a composite conductor for the ground wires. Carson has shown that the self impedance of the conductors is given by the expressions

$$Z_a = r_a + j.004657f\log \frac{D_{aa}}{G.M.R._a} + .004044f(P+jQ) \qquad (2\text{-}1)$$

ohms/mile

$$Z_g = r_g + j.004657f\log \frac{D_{gg}}{G.M.R._g} + .004044f(P+jQ) \qquad (2\text{-}2)$$

ohms/mile

where log is the logarithm to the base ten

and the mutual impedance between the two circuits is given by

Parallel Conductors
with Earth Return

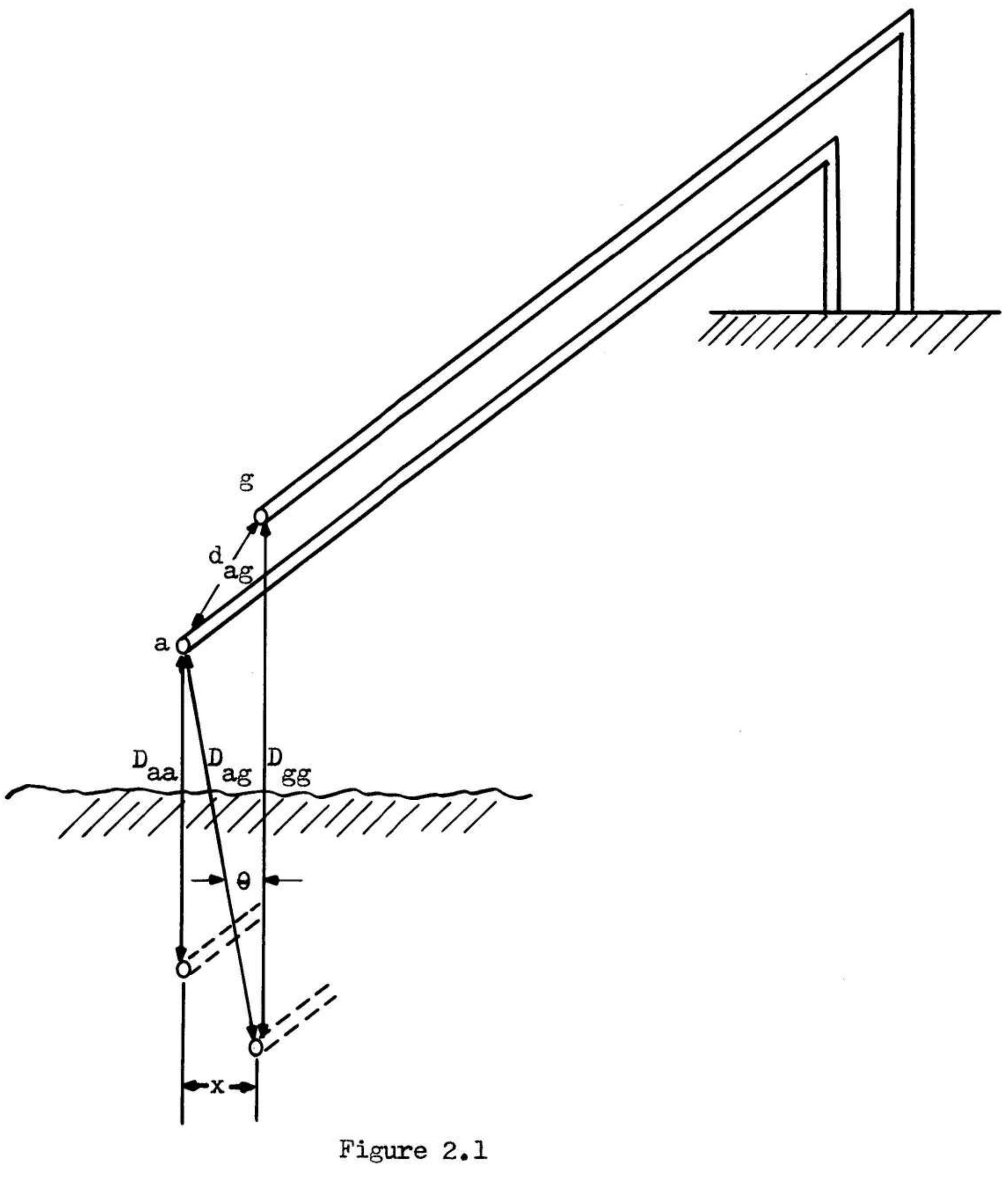

Figure 2.1

$$Z_{ag} = j.004657f\log \frac{D_{ag}}{d_{ag}} + .004044f(P+jQ) \qquad (2\text{-}3)$$

ohms/mile

where for both the self and mutual impedances the first terms are those that would be calculated for a perfect earth (earth resistivity equal to zero) and the (P+jQ) factors are corrections for a resistive earth. The (P+jQ) are infinite series resulting from a Bessel function solution of Carson's field analysis. The arguments of (P+jQ) are termed by Wagner and Evans as (p,θ) where for the self impedance

$$p = 8.565 \times 10^{-4}\, D_{aa} \sqrt{f/\rho}$$

or (2-4)

$$p = 8.565 \times 10^{-4}\, D_{gg} \sqrt{f/\rho}$$

and

$$\theta = 0 \qquad (2\text{-}5)$$

and for the mutual impedance

$$p = 8.565 \times 10^{-4}\, D_{ag} \sqrt{f/\rho} \qquad (2\text{-}6)$$

$$\theta = \sin^{-1} x/D_{ag} \qquad (2\text{-}7)$$

Here the coefficients assume D_{ag}, D_{aa} and D_{gg} are in feet, ρ is in ohm-meters and f is in Hertz.

As is generally true with Bessel functions the form of the series used is a function of the magnitude of the argument. For this reason Carson divided the solution into three regions of p, i.e., $p < .25$, $.25 < p < 5.0$ and $p > 5.0$. Wagner and Evans demonstrated that for most power system calculations only the lowest range need be considered and further that the angle θ is always very near zero. In this region P and Q are given as

$$P = \pi/8 - 1/3 \sqrt{2}\ p \cos\theta + p^2/16 \cos 2\theta\,(0.6728 + \ln 2/p)$$

$$+ p^2/16\ \theta \sin 2\theta \qquad (2\text{-}8)$$

$$Q = -0.0386 + 1/2 \ln 2/p + 1/3 \sqrt{2}\ p \cos\theta \qquad (2\text{-}9)$$

They further demonstrate that only the first term of P and the first two terms of Q need be considered to have less than a four percent error in evaluating P and Q. Then by a judicious combination of log terms they produce

$$Z_a = r_a + .00159f + j.004657f\log \frac{2160\sqrt{\rho/f}}{G.M.R._a} \quad \text{ohms/mile} \qquad (2\text{-}10)$$

$$Z_g = r_g + .00159f + j.004657f\log \frac{2160\sqrt{\rho/f}}{G.M.R._g} \quad \text{ohms/mile} \qquad (2\text{-}11)$$

$$Z_{ag} = .00159\ f+j.004657f\log \frac{2160\sqrt{\rho/f}}{d_{ag}} \quad \text{ohms/mile} \qquad (2\text{-}12)$$

which are known as the simplified Carson's equations. The term $2160\sqrt{\rho/f}$ is generally referred to as the equivalent depth of current return and denoted as D_e.[10,22,23]

It should be noted that for this condition the effect of conductor height disappears. For this reason the simplified equations are sometimes referred to as Carson's equations for conductors at ground level. Actually this form is just a fortunate coincidence of the range of parameters being considered.

Care should be taken to use the simplified equations only when p is less than .25. Assuming a maximum average conductor height of 100 feet then the maximum frequency at which these equations can be applied is

$$p = 8.565 \times 10^{-4}\ (200)\ \sqrt{f/\rho} \qquad (2\text{-}13)$$

$$p^2 = 73.5 \times 10^{-8} \times 4 \times 10^4 \; f/\rho \tag{2-14}$$

$$f = 34\rho \; p^2 \tag{2-15}$$

setting p at .25

$$f = 2.12 \; \rho \tag{2-16}$$

Therefore, for $\rho = 10$, maximum f = 21.2 Hz (2-17)

for $\rho = 100$, maximum f = 212 Hz (2-18)

for $\rho = 1000$, maximum f = 2120 Hz (2-19)

Above these frequencies the second region of p ($.25 < p < 5.0$) should be used. In this region the series form of P and Q become more complex and usually the curves given in Figure 2.2 and Figure 2.3 are used. Again making use of equation (2-15) with p set at 5.0 the maximum value of f for which these curves should be applied is (height = 100 feet).

for $\rho = 10$, maximum f = 8480 Hz (2-20)

for $\rho = 100$, maximum f = 84,800 Hz (2-21)

for $\rho = 1000$, maximum f = 848,000 Hz (2-22)

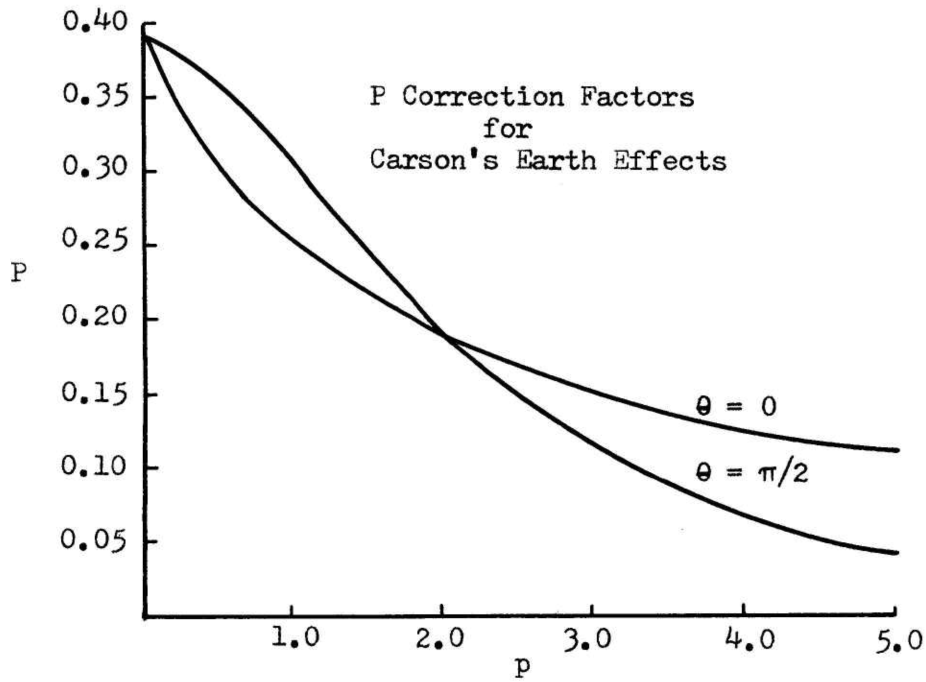

Figure 2.2

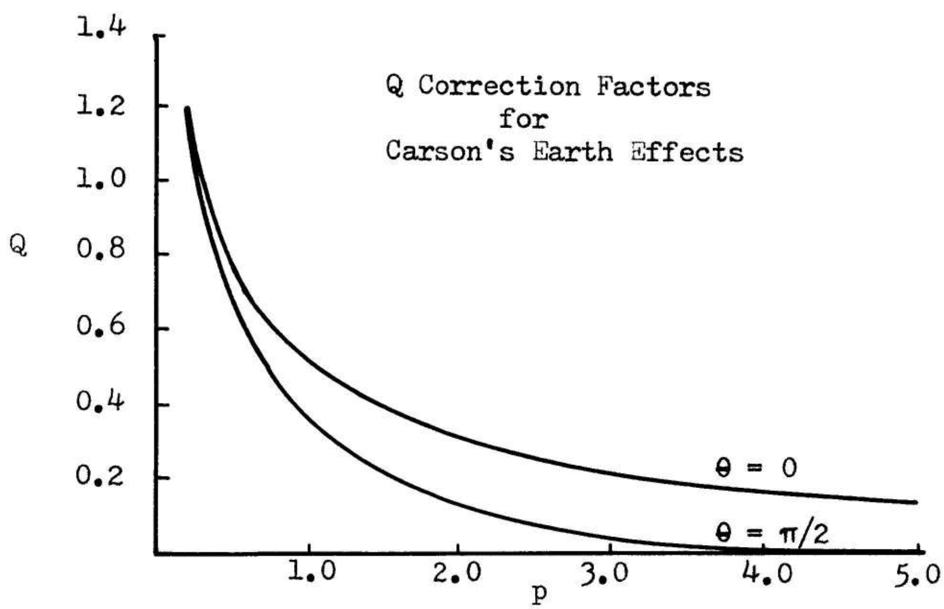

Figure 2.3

2.2 Physical Consideration of the Earth Effect

Carson's work only makes two simplifying assumptions that have proven to be valid through years of experience. These assumptions are that the earth is infinite in extent and uniform in conductivity and the current only flows in the earth parallel to the conductor. Some work has been done on stratified layers but the uniform conductivity approach seems sufficiently accurate for most power system work.[24] The assumption of only parallel current essentially ignores end effects. Thus the simplfied equations predict an infinite inductance at zero frequency since the effective depth of return (D_e) goes to infinity as f goes to zero. However, if one considers two probes placed on a semi-infinite conductive media x feet apart, intuitively the expected mean current depth would be less than the distance x. Therefore extending that argument to a transmission line we have

$$D_e = 2160\sqrt{\rho/f} < x \qquad (2\text{-}23)$$

for a line 50 miles long we get

$$2160^2\ (\rho/f) \leq (5280(50))^2$$

or

$$f \geq 6.63 \times 10^{-5}\ \rho \qquad (2\text{-}24)$$

Even for ρ = 1000 we see that end effects are of no real importance until f gets less than .1 Hz. Such a low frequency is well below the range of interest here.

To develop an insight for the effect of the conductor with earth return consider the simplified equations (2-10, (2-11) and (2-12). As the frequency increases the effective depth of return decreases. This process is very much like the "skin effect" problem where the penetration depth is a function of the frequency and the conductivity of the material. Therefore the inductance of a wire over earth decreases with frequency (encloses a smaller loop) while the resistance increases with frequency (has less parallel paths to follow.)

If the typical constants of the earth (conductivity=10^{-2} and permeability = $4\pi \times 10^{-7}$) are used in the skin depth equation at 60 Hz, the resultant skin depth is 650 meters or 2120 feet. Substituting the same numbers into D_e gives 2780 feet as the depth of earth return. The close correlation of these distances combined with the fact that they both have the same frequency dependence strongly suggest that the effect of magnetic diffusion in metals may be a very precise method to model the earth effect.

2.3 TLM Model of Earth Effects

The mathematical manipulation to derive Z_{oo} of Figure 1.3 was explained in Mr. Schmidt's thesis. Here we will only attempt to show how this impedance element is related to Figure 2.1. To actually calculate the frequency dependent parameters a computer program developed by Professor G. L. Wilson has been used.[25]

The circuit shown in Figure 2.1 can be redrawn schematically as shown in Figure 2.4a. When conductor "g" is the ground wire as is the case of interest the circuit is represented as shown in Figure 2.4b. To develop an understanding for how L_{oo} and R_{oo} vary with frequency consider the parallel combination of the ground wire impedance and the mutual impedance between the conductor and the ground wire as a good approximation of Z_{oo}. To simplify the analysis as much as possible consider an earth resistivity of $\rho = 1000$ so that the simplified form of Carson's equation will be valid through the frequency range of interest. Thus

$$Z_{oo} = \frac{(r_g + j0.004657f\log(d_{ag}/GMR_g)\ (.00159f + j0.004657f\log(D_e/d_{ag})}{r_g + .00159f + j0.004657f\log\ (D_e/GMR_g)} \tag{2-25}$$

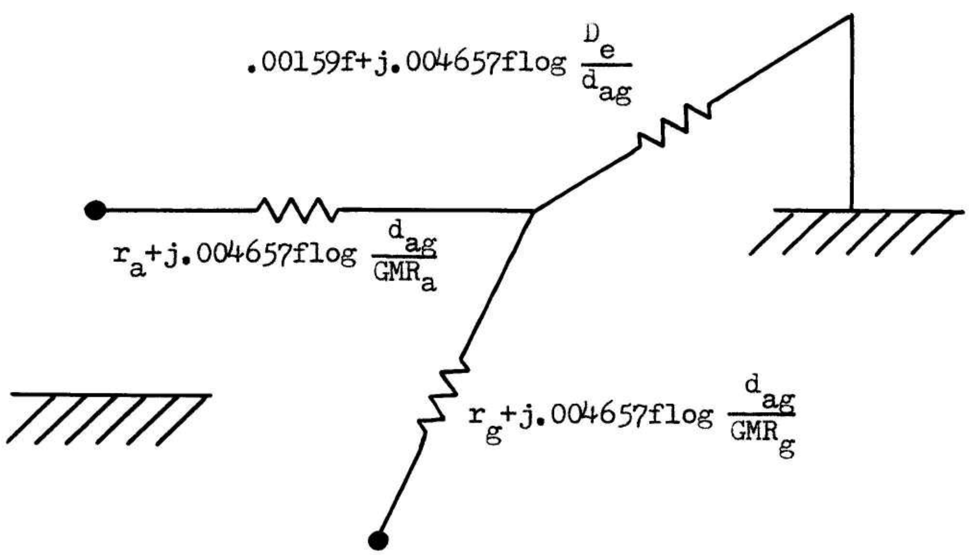

Equivalent Circuit of Two Conductors with Earth Return

Figure 2.4a

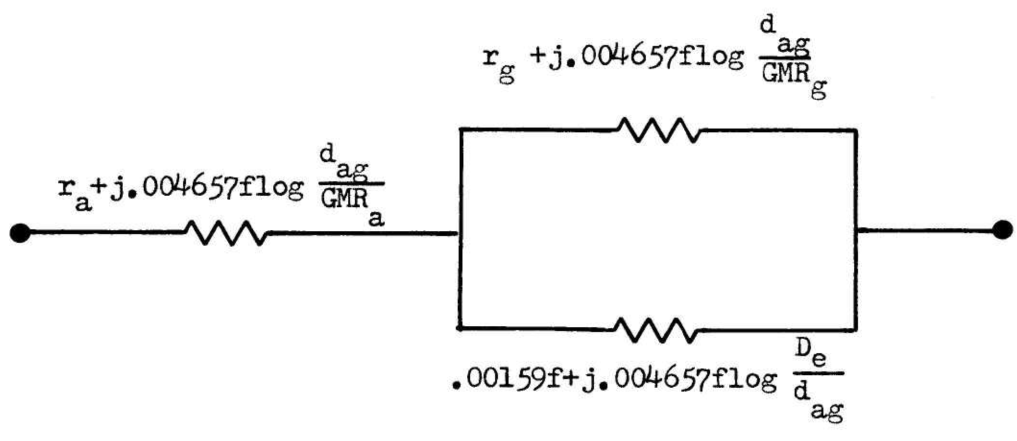

Equivalent Circuit of a Conductor with
a Ground Wire and Earth Return

Figure 2.4b

Conjugating and grouping into real and imaginary terms

$$Z_{oo} = R_{oo} + j\ 2\pi f\ L_{oo} \tag{2-26}$$

where

$$R_{oo} = \frac{1}{K}\ (r_g + .00159f)RR + .004657f\log \frac{D_e}{GMR_g}\ XX) \tag{2-27}$$

$$L_{oo} = \frac{1}{2\pi fK}\ (r_g + .00159f)XX - .004657f\log \frac{D_e}{GMR_g}\ RR) \tag{2-28}$$

$$K = (r_g + .00159f)^2 + (.004657f\log \frac{D_e}{GMR_g}\ )^2 \tag{2-29}$$

$$RR = .00159\ f\ r_g - (.004657f)^2\ \log \frac{d_{ag}}{GMR_g}\ \log \frac{D_e}{d_{ag}} \tag{2-30}$$

$$XX = .00159f(.004657f\log \frac{d_{ag}}{GMR_g}) + r_g(.004657f\log \frac{D_e}{d_{ag}}\ ) \tag{2-31}$$

also

$$Q_{oo} = \frac{(r_g+.00159f)XX - .004657f \log \frac{D_e}{GMR_g}}{(r_g+.00159f)RR + .004657f \log \frac{D_e}{GMR_g}} \tag{2-32}$$

These equations make it obvious why a digital computer is used to gain the solution. Only in the limits can R_{oo} and L_{oo} easily be evaluated. At zero frequency R_{oo} goes to zero and L_{oo} goes to infinity. At infinite frequency R_{oo} goes to infinity and L_{oo} appears to go to zero. Of course at high frequency, above 3000 Hz, these equations are in error but the trend is indicated. In the region of 100 to 1000 Hz a transition from earth to ground wire dominance in the effective resistance takes place. For a detailed example of how these parameters vary with frequency see Figure 2.5. Since skin effect in the conductors was computed by the computer program, the results of Figure 2.5 will be modified somewhat at higher frequencies from that predicted by equations (2-27), (2-28) and (2-32).

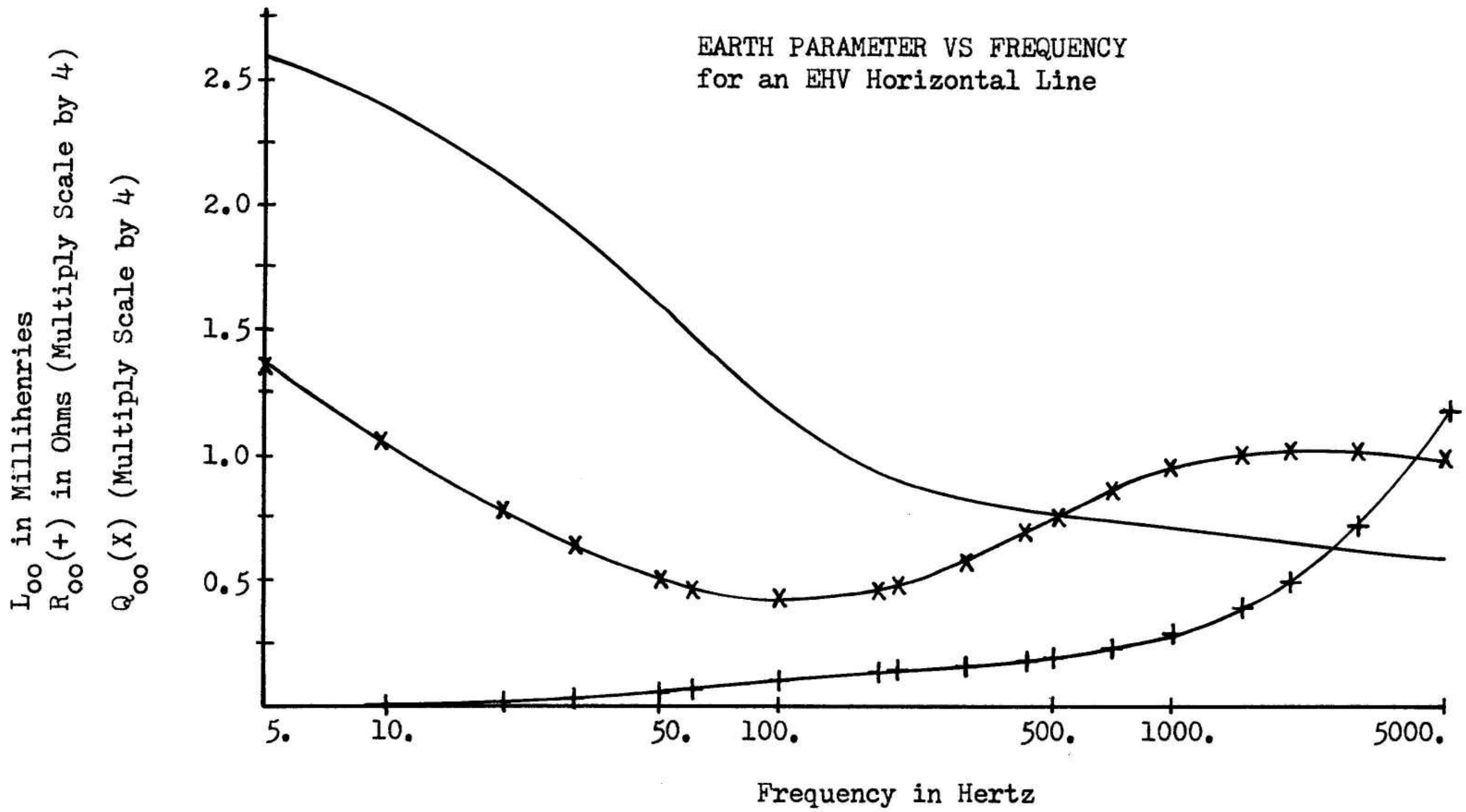
EARTH PARAMETER VS FREQUENCY
for an EHV Horizontal Line
L_{oo} in Millihenries
$R_{oo}(+)$ in Ohms (Multiply Scale by 4)
$Q_{oo}(X)$ (Multiply Scale by 4)
2.5
2.0
1.5
1.0
0.5
5.
10.
50.
100.
500.
1000.
5000.
Frequency in Hertz

Figure 2.5

CHAPTER 3

SIMULATION OF FREQUENCY DEPENDENT IMPEDANCE USING DIFFUSION

From the discussion in Chapter 2 it becomes clear that the frequency characteristic of the Z_{00} impedance is primarily due to the diffusion characteristic of the earth. As the frequency increases the current cannot penetrate as deeply into the earth therefore the effective return path is raised closer to the surface of the earth. Thus the inductance of the transmission line decreases because the effective area of the loop formed by the transmission line and its return path are diminished.

3.1 A Long Solenoid Approach

To model such nonlinear impedance it is logical to make use of the diffusion phenomena. By making an inductive loop around a solid metallic volume the inductance of the loop will diminish as frequency increases due to the diffusion phenomena. A detailed analysis of this effect is shown in Appendix A. It can be seen for this long solenoid model the inductance decreases with increasing frequency. For this case it varies inversely with the square root of frequency. However this inductance is modified by a rather complicated Bessel function $(\overline{U})$. Figure 3.1 shows a plot of this Bessel function modifier as a function of its argument. Similarly from Appendix A it can be seen the AC resistance is a function of the square root of frequency and

Bessel Modifiers of the Continuum Equations of Inductance
and Resistance for a Metallic Core Solenoid

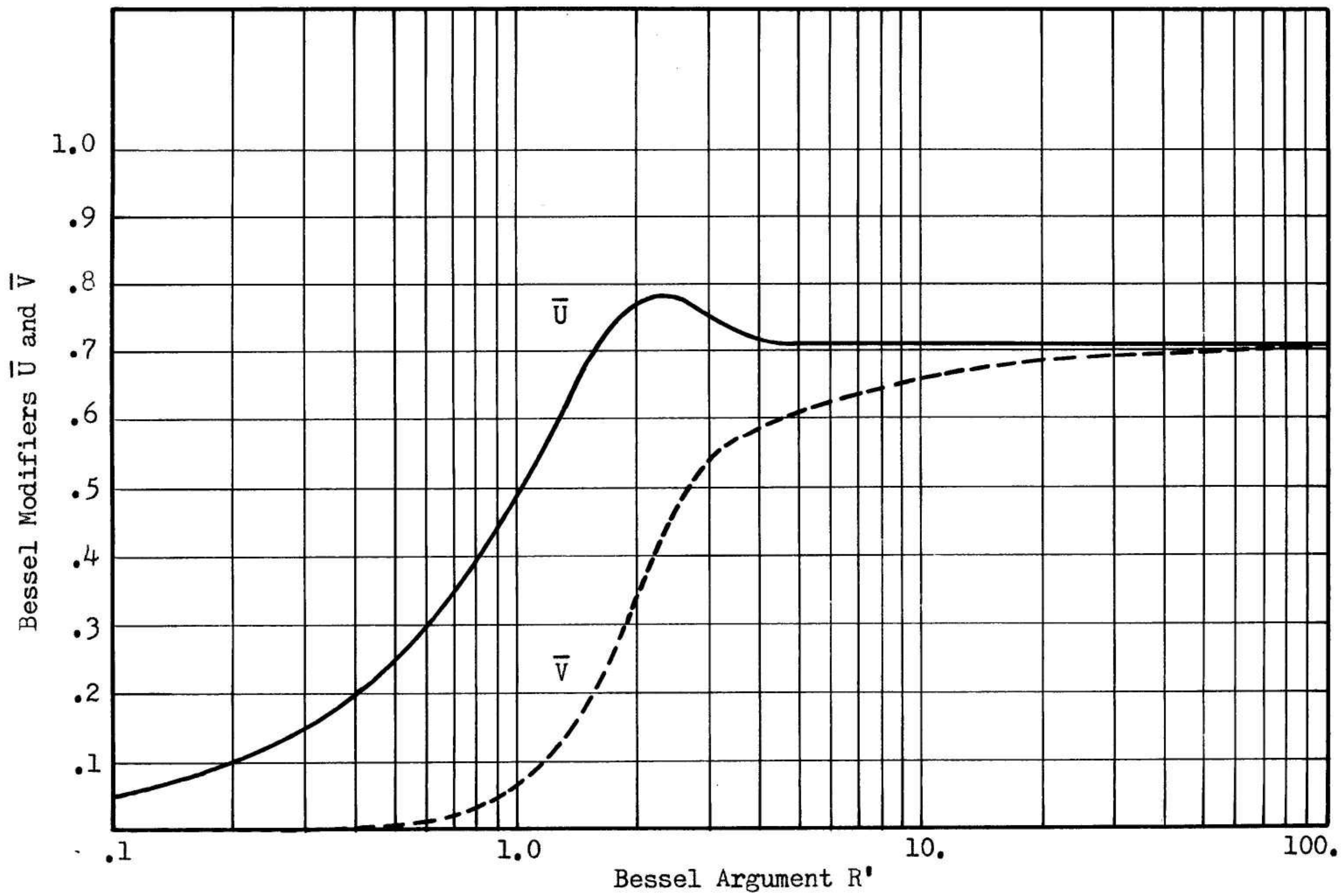

Figure 3.1

it is modified also by another complex Bessel function $(\overline{V})$. Figure 3.1 also shows this modifier plotted as a function of its argument. For values of the argument above 10 the reactance characteristic of L becomes equal to the resistance r_s. Therefore Q goes to 1 for this type of model at higher values of the Bessel function argument.

The argument of the Bessel functions is dependent on four terms, i.e., the conductivity of the material, the permeability of the material, the radius of the solenoid, and on the frequency applied to the coil. Therefore to gain an inductance that decreases with frequency starting at a very low frequency, it is necessary to properly choose the conductivity and permeability of the metal and its radius. Inspecting the lower end of the characteristic shown in Figure 3.1, it can be seen that the inductive multiplier essentially varies as the square root of frequency. Until the argument departs from this portion of the curve the inductance of the coil will remain constant. When the Bessel modifier no longer increases as the square root of frequency, the coefficient that is decreasing as the square root of frequency will become dominant. From Figure 3.1 it can be seen this decrease of inductance will start at a value of approximately 1.2 and will actually decrease more rapidly than one over the square root of frequency between 2.2

and 4.0. Hereafter the Bessel modifier becomes constant and the rate of decrease in inductance will stabilize at exactly one over the square root of frequency.

3.1.1 A Copper Rod Solenoid

To test the validity of this analysis, a coil was wrapped on a rod of copper 3.5 centimeters in diameter and 15 centimeters long. For ease of measurement 1000 turns of No. 16 wire were wrapped on the rod. Figure 3.2 gives the results of this test as test points of measured inductance vs frequency.

The expected response of this coil to frequency variation can be computed from equation (A-15) and the $\bar{U}$ curve of Figure 3.1. Thus

$$R' = \sqrt{\omega \mu \sigma}\ R \tag{A-15}$$

gives

$$f = (R')^2 / 2\pi \mu \sigma R^2 \tag{3-1}$$

From equations (3-1) and for the argument (R') of 1.2 the break frequency is 10 Hz (for copper $\sigma = 5.9 \times 10^{+7}$ and $\mu = 4\pi \times 10^{-7}$). The break frequency is the point where the inductance starts to decrease with frequency. Since the Bessel

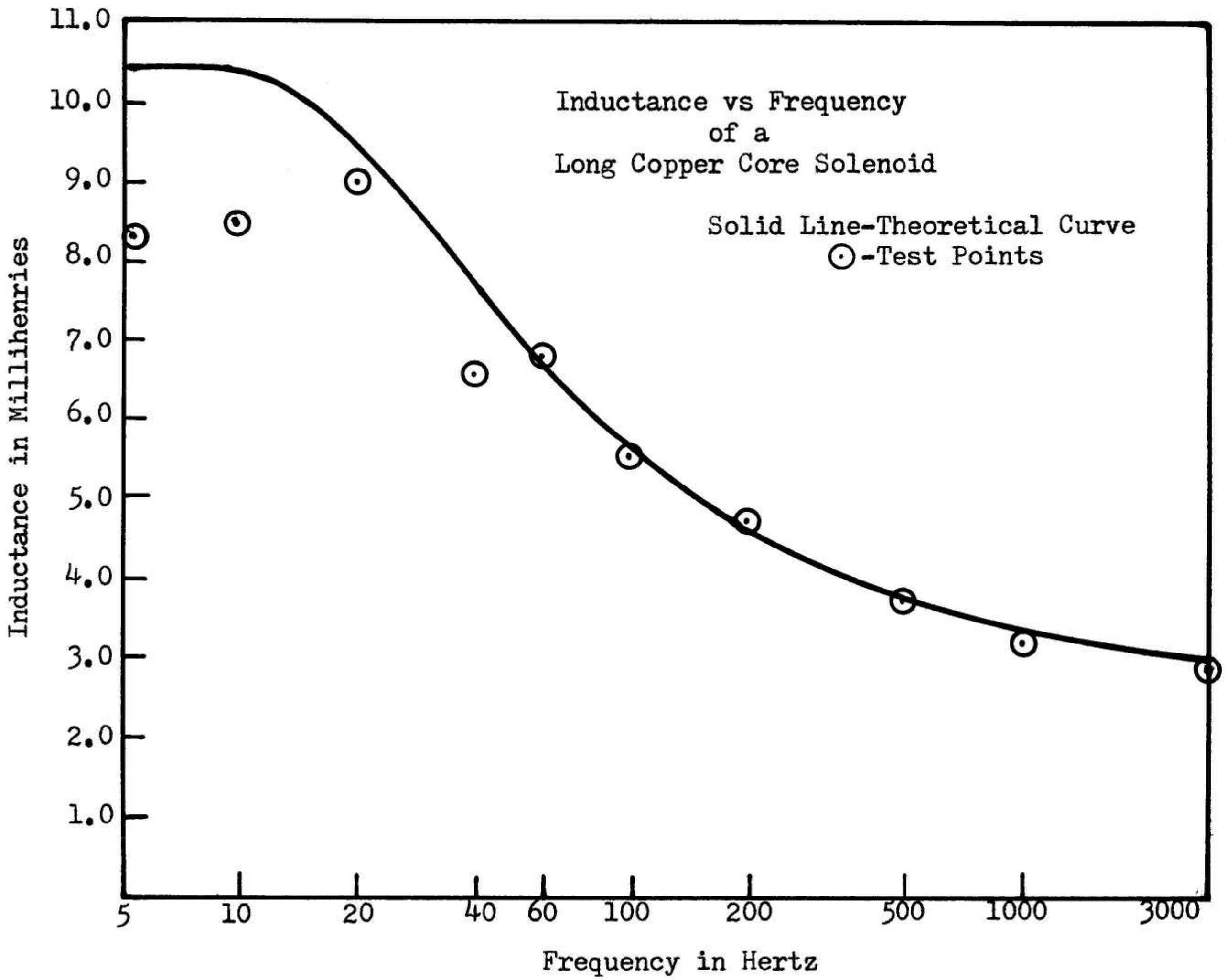
Inductance vs Frequency
of a
Long Copper Core Solenoid
Solid Line-Theoretical Curve
-Test Points
Inductance in Millihenries
11.0
10.0
9.0
8.0
7.0
6.0
5.0
4.0
3.0
2.0
1.0
5
10
20
40
60
100
200
500
1000
3000
Frequency in Hertz

Figure 3.2

modifier decreases for values of the argument between 2.2 and 4.0 the maximum decrease in inductance will occur in the range of frequencies from 34 to 113 Hz.

When adjustments are made for the added linear inductance due to winding build-up, the frequency characteristic of the coil is very close to that predicted by the theory. This is demonstrated by the solid curve in Figure 3.2. The test points at the low frequencies of 5 and 10 Hz were lower than that predicted. It is believed that since the impedanced angles measured at these points were only 3.6 and 7.2 degrees respectively, an error in measurement of one degree could account for the apparent disparity.

The resistance characteristic of the coil was found to also be in very good agreement with that predicted by the theory. However the DC resistance of the wire dominated the resistance through to 100 Hz. This combined with the effect of the added linear inductance due to winding build-up caused the Q of the coil to increase throughout the frequency range measured.

3.1.2 Ferromagnetic Rod Solenoids

From the work on the copper solenoid it was concluded that to gain the desired results a method must be found to drastically reduce the number of turns required. Since the impedance varies as the square root of permeability and inversely as the square root of conductivity, it was concluded that a form of ferromagnetic rod should be used. By adjusting the radius of the rod the argument of the Bessel modifier could be held to an advantageous range and yet considerable gain could be achieved from the square root of the ratio of permeability to conductivity. This was an unfortunate observation.

After a great deal of testing on various ferromagnetic materials it was found that the diffusion equation as derived in Appendix A is only applicable to nonferromagnetic metals. All existing ferromagnetic metals exhibited a highly nonlinear relative permeability with respect to the ampere-turns.

To demonstrate how this nonlinear nature of permeability in ferromagnetic materials invalidates the classical diffusion equation, the steps taken to derive the diffusion equation are repeated here. First consider Maxwell's equations for a magnetoquasistatic system.

$$\nabla \times H = J \qquad (3\text{-}2)$$

$$\nabla \cdot B = 0 \qquad (3\text{-}3)$$

$$\nabla \times E = -\frac{\partial B}{\partial t} \qquad (3\text{-}4)$$

from Ohm's law

$$J = \sigma E \qquad (3\text{-}5)$$

we get by substituting into (3-4)

$$\frac{1}{\sigma} \nabla \times J = \frac{-\partial B}{\partial t} \tag{3-6}$$

now substituting (3-2) into (3-6)

$$\frac{1}{\sigma} \nabla \times (\nabla \times H) = -\frac{\partial B}{\partial t} \tag{3-7}$$

making use of a vector identity

$$\nabla(\nabla \cdot H) - \nabla^2 H = \nabla \times (\nabla \times H) \tag{3-8}$$

equation (3-7) becomes

$$\frac{1}{\sigma} (\nabla(\nabla \cdot H) - \nabla^2 H) = -\frac{\partial B}{\partial t} \tag{3-9}$$

It is at this point that the assumption of permeability independent of H is usually made. By multiplying and dividing the left side of the equation by μ the classical diffusion (A-2) is obtained. This is a valid operation only when μ is constant. If, for example, the permeability has the relatively simple form of

$$\mu = \alpha \left(1 + \alpha_1 H^2\right) \tag{3-10}$$

where α and α_1 are constants, it is no longer possible to move the permeability term through the vector operations. Thus the first term on the left of equation (3-9) no longer vanishes by virtue of (3-3) and the term on the right produces three terms when the partial derivative with respect to time is taken. Actually an exact equation for permeability would be much more nonlinear than (3-10) if saturation were represented.

After spending considerable time attempting to find a ferromagnetic material that could be treated as though it had a constant permeability, it was discovered that recent researchers in the area of electromagnetic interference shielding had been much more successful in predicting the performance of solid ferromagnetic materials by treating the permeability as highly nonlinear.[26,27,28] Unlike many researchers, both present and past, who have usually assumed they measured the permeability of the material incorrectly when they were trying to use a diffusion equation to predict this penetration characteristic, Young and Ferber approached the problem by assuming the flux density to be zero for zero H and a very high level for any finite H.

It could be argued that time should be spent to solve the nonlinear equations to see if a characteristic similar to that of Appendix A would develop. However a second phenomena can be observed that demonstrates the fruitlessness of this approach. Since the relative permeability of ferromagnetic material is a function of the ampere-turns applied, any coil designed using a ferromagnetic material would be sensitive to the current through the coil. The long air gap approach[29] used to linearize such nonlinear magnetic circuits does not work because the break in characteristic with respect to frequency is a function of the permeability. Since it is required that the coil designed be independent of ampere-turns from 0 to 1 ampere, it would be impossible to meet this requirement with any known ferromagnetic material.

3.2 Copper Disk in the Air Gap of a Ferromagnetic Yoke

By reviewing the equations developed in Appendix A it was observed that the long solenoid constraint is made to guarantee an axial magnetic field and to control the magnetic path for integrating around the H•dl contour. If it were possible to close the flux path around a short solenoid through some infinitely permeable material, the long solenoid constraint would no longer be necessary. Furthermore, it was observed that the inductance characteristic would be greatly increased if the length of the solenoid could be reduced, i.e., the inductance is inversely proportional to the length of the solenoid.

The short solenoid was accomplished by placing a thin disk of copper between the pole faces of a magnetic yoke. Since it is desired to have only the copper controlling the diffusion characteristics, the magnetic portion of the circuit must be laminated very finely in order not to interfere with the flux distribution. For a first attempt at this type of solution, two Silectron C cores were used with an air gap total of approximately 100 milli-inches (50 mils air and copper between each pole face of two C cores.)[30] This much separation was used because the Silectron material still exhibits an extremely nonlinear permeability characteristic with respect to ampere-turns/meter. Therefore all the ampere-turns had to be absorbed in the air gap and very little in the ferromagnetic yoke.

More testing showed the equations of Appendix A did not accurately predict the radius of copper required between the pole faces. It was observed that as the distance between pole faces was diminished, the accuracy of the equations improved yet the ampere-turn error became unacceptable. Analyzing this circuit revealed again trouble was being encountered with the ferromagnetic nonlinearities. As the frequency is increased the only flux passing through the copper disk is at the edges of the disk since the counter flux being produced by circulating currents is excluding flux from the center. As it moves to the edge of the disk the effective flux density at the center of the disk goes to zero. In this region the ferromagnetic yoke has its permeability go to that of free space since it is dependent on the flux density. This in effect increases the air gap in the vicinity of the center of the disk. Under these circumstances it is easier for the counterflux being produced by the diffusion characteristic to close on itself, i.e., back through the copper disk rather than return through the yoke circuit as was originally intended. The result is an increase of flux density at the perimeter of the yoke material and no net decrease in total flux linkage through the magnetic circuit. Since the coil is wrapped on the yoke, there is no appreciable decrease in inductance until the flux is forced into the fringing fields. At this point the circuit demonstrates a characteristic similar to that discussed under the Copper Solenoid section.

Since this magnetic yoke circuit was found unsatisfactory due to nonlinearities of the magnetic circuit with respect to ampere-turns, it was decided to try a powdered iron yoke material. The characteristics of powdered iron materials are relatively unaffected by ampere-turns.[31,32] This fact allowed the use of much smaller air gaps and therefore much thinner disks of copper material. It was found upon testing two different manufacturers' powdered iron materials[31,32] that very close correlation existed between the frequency response predicted by Appendix A and that measured as long as the disk did not extend beyond the mid-point of the window.

As soon as the disk increased beyond this point the inductance characteristic did not start to fall with frequency as soon as predicted. This phenomena is a function of the nonlinear effect of extremely long fringing fields, i.e., the fields after a point tend to close back on the same U core rather than pass through the copper into the other side. It was not possible to make measurements on these fields to determine their direction because of their very low levels. However, this was logically deduced by using a larger window area powdered iron material and finding the agreement increased until the disk material again exceeded one half of the window area. For certain transmission line models it would be desirable to have even larger powdered iron yokes; however, the cost of such yoke would be prohibitive. This will be discussed further in Chapter 4.

CHAPTER 4

DESIGN OF FREQUENCY DEPENDENT R, L AND Q

As was demonstrated in Chapter 3 the combination of powdered iron yokes and copper disks gave a frequency dependent inductance and resistance. However, in this form the inductance and resistance characteristic is not very close to that required by the actual Z_{oo} parameter. Referring to Figure 2.5 for a horizontal 765 kV line it can be noted that the inductance characteristic produced by this copper disk circuit falls off far too rapidly with frequency. Also the Q characteristic of the circuit reaches its minimum value very soon after the initial break from constant inductance occurs (in about a decade of frequency.) Thus if the minimum point in the Q curve of Figure 2.5 is to be matched by a disk circuit the R' of Figure 3.1 must be adjusted so the disk circuit Q will approach unity at this point in frequency. By adding a linear inductor in series with the disk circuit to reduce the rate of overall inductive fall-off, a minimum Q point will be established. Therefore, from Figure 3.1, the minimum frequency at which the inductance characteristic can be matched will be less than a decade below the point of minimum Q, i.e., the inductance must be allowed to remain constant below this point. This establishes the criteria for deciding how large the disk radius should be and the lower frequency bound of the model.

Impedance vs frequency computations were made on 345 kV vertical and horizontal configuration lines and a 765 kV horizontal configuration line. It was found for all the horizontal configuration lines, the minimum Q point occurred at approximately 100 Hz and for the vertical configuration at approximately 25 Hz. Referring to Figure 3.1 and taking the point where the ratio of the inductance multiplier, $\overline{U}$, to the resistance multiplier, $\overline{V}$, approaches unity (the exact point chosen was $R' = 5.5$), it can be calculated from equation (A-15) that the radius of the copper disk required would be approximately one inch for the horizontal and two inches for the vertical.

As discussed in Chapter 2, ideally the Q of the circuit should be infinite at zero frequency. As a practical matter this is an impossibility since a coil of wire always has a finite resistance (excluding super-conductor considerations.) To minimize the effect of the resistance of the wire, No. 10 copper magnet wire was used. This allowed the Q to approach that required between 10 and 20 Hz. Therefore the combination of resistance of the winding and the point at which the inductance characteristic started to decrease with frequency set the lower bound for which this simulation could be considered to be an exact model of the system parameter. That bound is approximately 20 Hz.

This sets the characteristic of the coil design and yet it is necessary to match the curve through the whole frequency range (20 to 5000 Hz). As stated the inductance characteristic of these diffusion circuits falls off far too rapidly with frequency. Also the Q characteristic approaches unity above R' of 6.0. Both of these problems are solved by placing a linear inductor in series with the coil containing the copper disk. By adjusting the level of inductance of both coils it is possible to get a combined inductance characteristic which is very close to the inductance required by the Z_{oo} through the whole frequency range. By making the linear inductor an extremely high Q coil, as the inductance falls off in the disk coil a larger percentage of the total inductance is made up by the linear coil. Thus a point is reached where the Q of the circuit starts increasing again.

What appeared to be an arbitrary selection of R' (R' = 5.5) to match the minimum Q becomes more definite. The magnitude of the desired Q at the minimum point and the frequency at which it occurs plus the magnitude of inductance required constrains the dimensions of the metal disk very precisely. It is now necessary to decide which combination of the coils should be used to match a given characteristic. This could be done by a non-linear analysis. However for this case it is far simpler to actually calculate a characteristic for the inductor design containing the copper disk, hereafter called the E coil and choose a level of inductance for the linear coil, hereafter referred to as the G coil. By writing a very simple computer program, it is possible to take percentages of a base characteristic of both the E and G coils and add them to gain an array of possible combinations.

(A copy of this program is shown in Appendix B.) By scanning through the combinations, it was possible to narrow the search to just a few characteristics which appeared to fit. From these few characteristics the best overall fit of inductance and of resistance for the circuit was chosen.

The linear coil or G coil used in this design actually is not a linear coil. Referring to Figure 2.5, it can be seen that the Q characteristic at a high frequency of around 1000 to 2000 Hz tends to level out and actually drop off somewhat. If a purely linear high Q coil is used, the Q characteristic will not drop off but will continue to climb at the higher frequencies. To prevent this it is necessary to construct the linear coil similarly to the E coil. By designing the G coil with a much smaller radius disk so that its break frequency occurs at a much higher point, a second drop off in Q can be obtained. By looking at the Q requirements it is possible to select the diameter of disk required in these coils.

It was found the high frequency drop off in Q occurs at lower frequencies for the lower earth resistivity cases. Therefore the G coil must be designed with different radius disk for different resistivities. Since the resistance of a coil with the copper disk starts to increase faster than the inductance falls off, it is necessary to design the break point at the maximum Q point. Then the overall Q characteristic will exhibit the desired shape.

Since the disk required in the G coil for this final trimming of the Q is much smaller in radius, it was elected not to use copper in this instance but to use a metal called Phosphorbronze. It has a measured conductivity of 1.0×10^7 mhos/meter and is much more rigid than copper. Thus these small disks are less likely to be damaged in the handling required for changeovers from one characteristic to another. Table 4.1 gives the Phosphorbronze disk dimensions found necessary as a function of the earth resistivity. Table 4.2 gives a table of the E coil copper disk dimensions found necessary for the two different basic line configurations.

Table 4.1

G Coil Disk Dimensions and Associated Earth Resistivities

Disk Dimension		Earth Resistivity in Ohm-M		
Radius in Inches	Thickness in Inches	10	100	1000
0.47	0.005	X		
0.35	0.005	X		
0.275	0.005		X	
0.24	0.005		X	
0.20	0.005			X

Table 4.2

E Coil Disk Dimensions and Associated Line Configurations

Disk Dimensions		Line Configuration
Radius in Inches	Thickness in Inches	
1.0	0.010	Horizontal
1.5	0.020	Vertical

All the data presented are for yokes of Indiana General U-cores, Part# F-813-1 for the E coils and for the G coils Part# F-465-1. It would be possible to use Ferroxcube U cores, Part# 1F5 and a copper disk with a radius closer to the theoretical 2.0" required to gain a better fit for the vertical configuration lines. However, physically the Ferroxcube core is dimensionally twice that of the Indiana General core and more than twice as expensive as the Indiana General core. As will be shown in the next chapter it is doubtful the increased expense can be warranted.

CHAPTER 5

CONSTRUCTION OF THE G AND E COIL MODELS

The techniques presented in Chapter 4 were used to develop the electrical characteristic of the design. Because the diffusion phenomena was used, the desired electrical characteristic also set some of the physical characteristic of the coils. Other physical constraints were set by the phase portion of the TLM already well under construction.

Because the operating panels for the TLM had already been drilled and mounted with only six taps per coil, they specified the number allowed by this design. Tables 5.1 through 5.4 give the tap-turn values for the G and E coils for the 4 and 8 mile sections. In these tables only a fraction of total inductance of the coil is listed since the magnitude of the inductance at any given frequency is a function of the metallic disk used to separate the two U cores. For convenience, Figure 8.3 of Mr. Schmidt's thesis is reproduced here as Figure 5.1 with tap numbers assigned to the G and E coils.

The actual winding of the coils should be of the form shown in Figure 5.2. The G and E coils are to be mounted directly behind their respective tap positions as shown in Figure 5.1. A suggested clamping and mounting support is shown in Figure 5.3. This type of mounting should facilitate rapid changing of disk when required. Any mounting that is used must

Table 5.1

Number of Turns and Fraction of Total Inductance per Tap for the G Coil for a 4 Mile Section

Tap No.	Turns	Fraction of Total Inductance
1	30	.46
2	34	.57
3	37	.665
4	39	.725
5	43	.88
6	46	1.00

Table 5.2

Number of Turns and Fraction of Total Inductance per Tap for the E Coil for a 4 Mile Section

Tap No.	Turns	Fraction of Total Inductance
1	45	.525
2	47	.575
3	51	.675
4	53	.73
5	55	.79
6	62	1.00

Table 5.3

Number of Turns and Fraction of Total Inductance per Tap for the G Coil for an 8 Mile Section

Tap No.	Turns	Fraction of Total Inductance
1	42	.46
2	48	.57
3	52	.665
4	55	.725
5	61	.88
6	65	1.00

Table 5.4

Number of Turns and Fraction of Total Inductance per Tap for the E Coil for an 8 Mile Section

Tap No.	Turns	Fraction of Total Inductance
1	64	.525
2	67	.58
3	72	.675
4	75	.73
5	78	.79
6	88	1.00

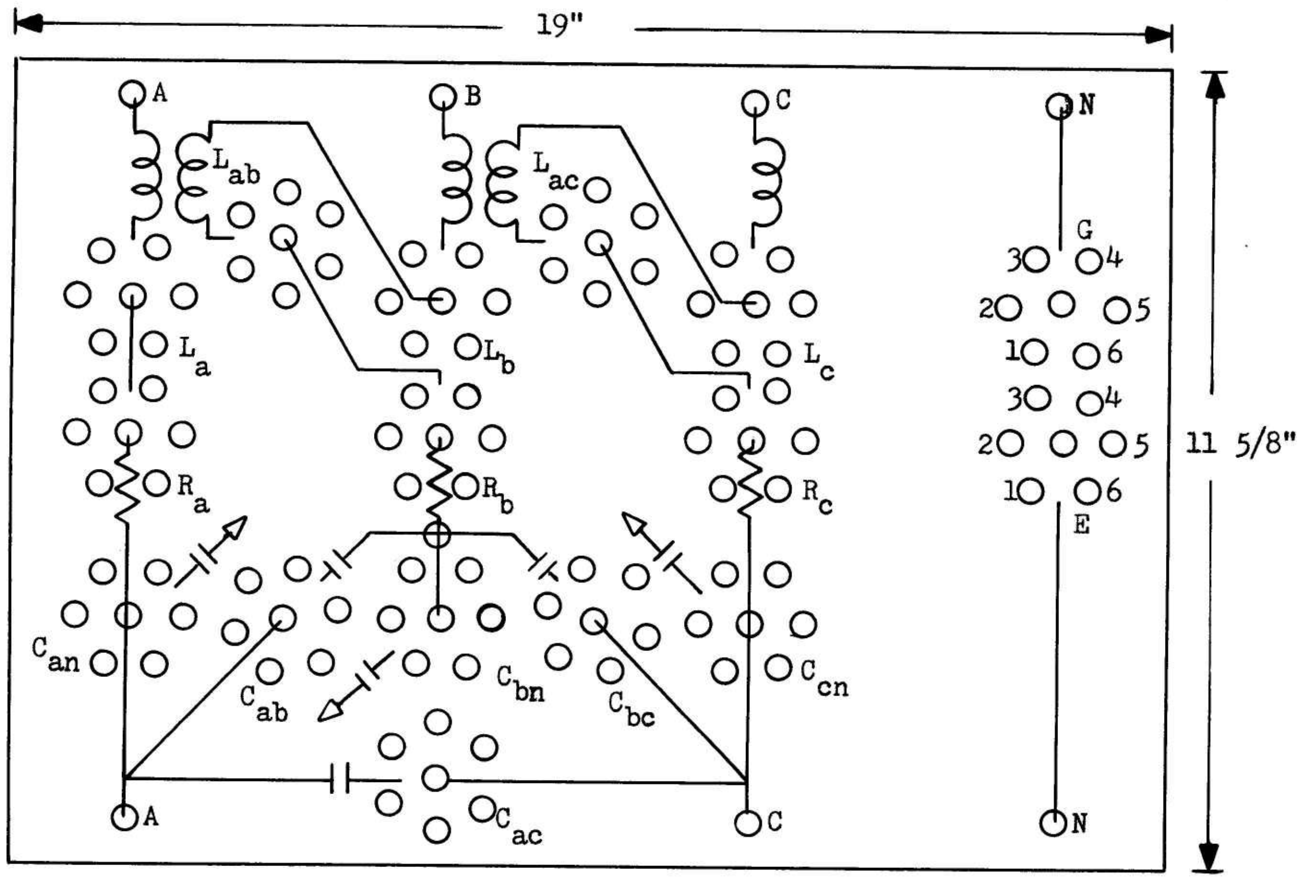

Operating Panel of Typical T.L.M. Section

Figure 5.1

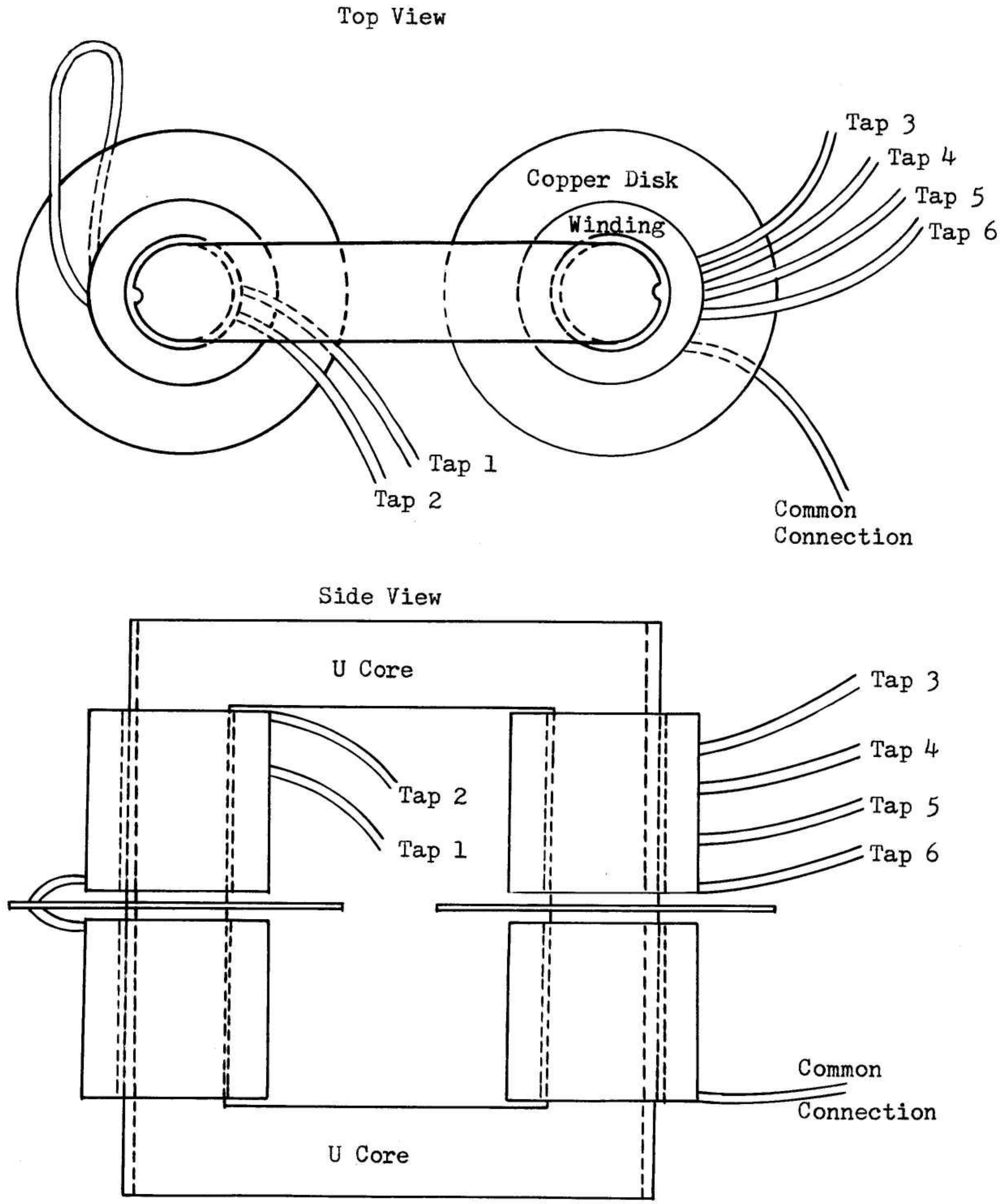

Winding Arrangement of E and G Coils

Figure 5.2

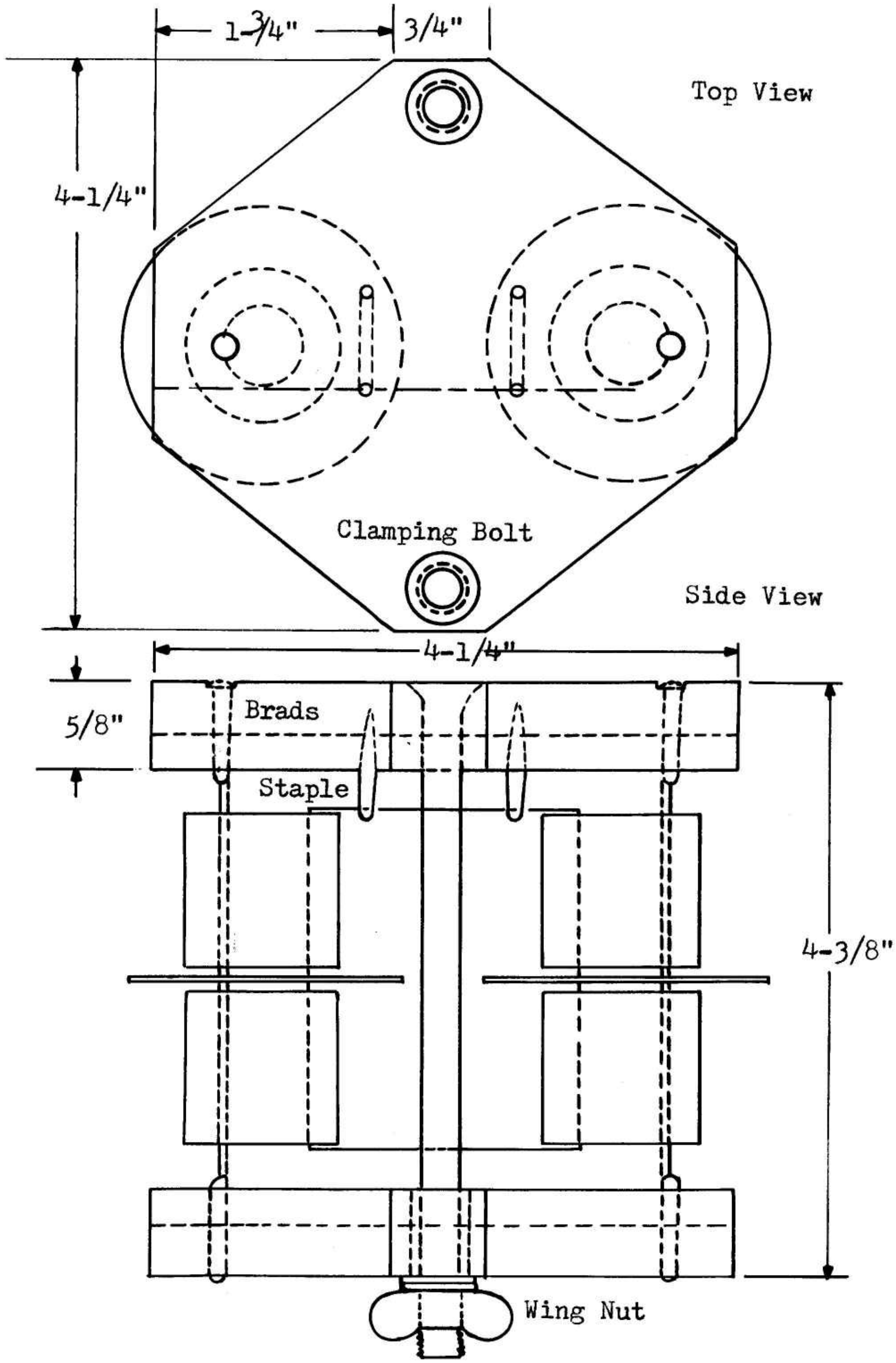

Mounting Frame for the E Coil
Figure 5.3

allow a minimum of six inches for the long dimension of the E coil and three inches for the G coil. There is sufficient room to undermount the E coil from the top shelf of the drawer. The G coil can be positioned on top of the top shelf.

The mounting frame shown in Figure 5.3 is designed for the E coil. A similar design can be made for the G coil by scaling down the dimension proportional to the core size. The brads shown will keep the cores from moving sideways when changing disk. The simple staples shown should securely hold the top core assembly in place. To make possible fine adjustment of the two U core pole faces, the bottom part of the mount should have the holes for the clamping bolts drilled 1/8" larger in radius than the bolt. This will allow a means for correcting any misalignment that may occur during construction.

All the data presented on the 4 mile sections are for coils wrapped with No. 10 magnet wire. For the 8 mile sections No. 12 wire could be used to achieve nearly the same results since the inductance will increase by 2 but the DC resistance will only increase by the $\sqrt{2}$. However as will be shown in Chapter 6 a better low frequency fit could be achieved if the DC resistance were held to a minimum. Also holding the winding resistance to as low a value as feasible will compensate for contact resistance inherent in "plugging up" a line simulation. Therefore unless winding hardships dictate otherwise, No. 10 wire should also be used on the 8 mile sections.

CHAPTER 6

VERIFICATION TEST

The E and G coils were built for a 4 mile section of the TLM as specified in Chapter 5. Each coil was tested separately and then the series combination was tested for R, L, and Q vs frequency. In addition each coil was tested for variation in inductance vs current through the coil. A summary of these tests and curves showing the match obtained with the line characteristics will be given in this chapter.

6.1 Current Sensitivity Test

The current sensitivity measurements were made at 60 Hz for both coils. Since for the Z_{oo} impedance there is really no base operating current (the base for the phase parameters was 38.6 ma), 20 ma was chosen as a base rather arbitrarily. Table 6.1 gives the percent deviation of the impedance from the impedance at 20 ma for the E coil. The one inch radius copper disk 10 mils thick was in place for the test.

Table 6.2 gives the percent deviation of the impedance from the impedance at 20 ma for the G coil. For this test 5 mil mylar spacers were used to separate the U cores.

The variation of the E coil is well within the allowed tolerances. Above 100 ma the G coil starts to exceed the +5 percent tolerance. Since the two coils are always to be used in series this error is not as significant as it first appears.

Table 6.1

Percent Deviation in Impedance vs Current for the E Coil at Top Tap

Current in Milliamps	Impedance Deviation in Percent
0.186	-5.5
3.54	-0.65
20.0	0.0
200.0	0.0
1000.0	+1.0

Table 6.2

Percent Deviation in Impedance vs Current for the G Coil at Top Tap

Current in Milliamps	Impedance Deviation in Percent
0.075	0.0
2.0	-1.0
20.0	0.0
106.0	+5.0
425.0	+15.0
1000.0	+20.0

For the most unfavorable combinations of G and E coils taps, the combined error is +12 percent at 1.0 amperes. For a typical combination the error is approximately +6 percent at 1.0 amperes. Since the typical error at the maximum current is just outside of the tolerance the combined design is considered acceptable.

6.2 R, L, and Q vs Frequency Test

The circuit used to test the coils is shown in Figure 6.1. The oscilloscope was triggered from the oscillator so that phase shift measurement could be made. The data recorded at each frequency was the current through the resistor (voltage across it divided by the resistance) voltage across the coil and the shift between them. The shift was measured and recorded as the number of grading divisions on the scope face. For convenience the scope was set to sweep one full cycle at each frequency. The computer program listed in Appendix C was used to compute the individual R and L at each frequency and to combine them to give the resulting Z_{oo} representation.

Figures 6.2 through 6.9 give representative samples of the fits obtained for the line configurations considered. The R, L, and Q's shown on the curves are the points obtained from these tests. The solid curves are plotted directly from the results of Professor Wilson's program. As can be seen the horizontal lines are generally matched very well. The Q fit for the vertical lines is low in the 60 to 180 Hz range as would be

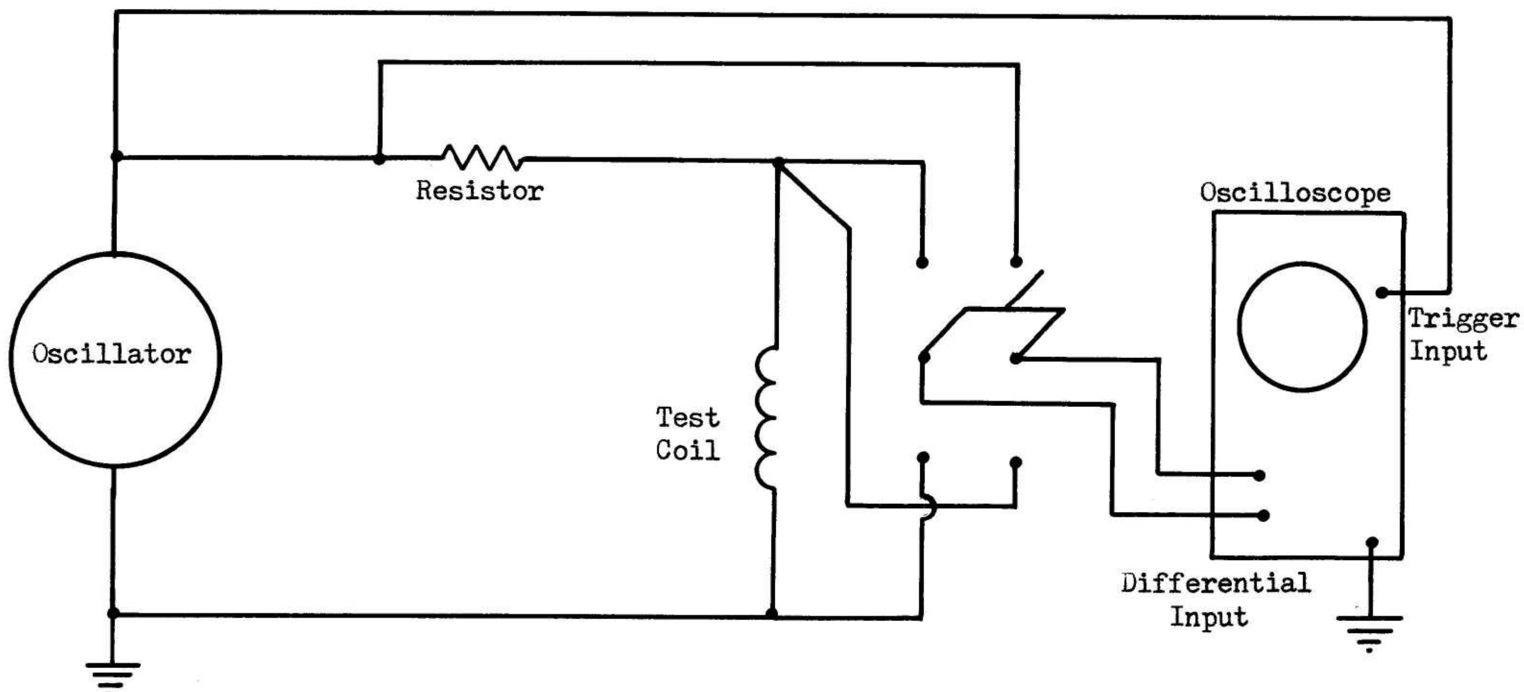

Test Circuit for Making Impedance vs Frequency Measurements

Figure 6.1

EARTH PARAMETERS VS FREQUENCY
765 kV AEP HORIZONTAL ALUMINUM TOWER
Earth Resistivity = 10 Ohm-M
4 Mile Sections Scaled by 0.355 Ohms/Ohm

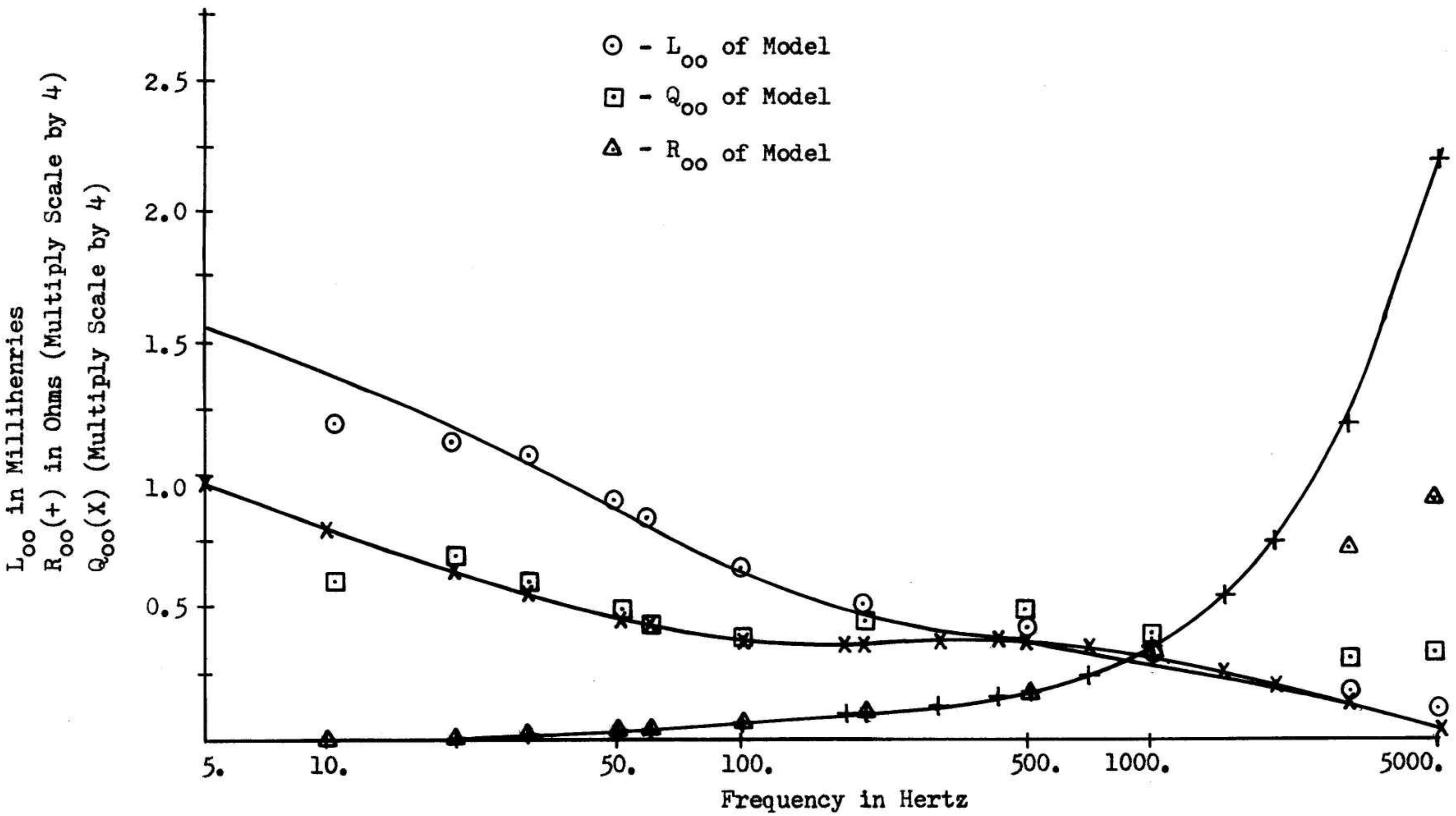

Figure 6.2

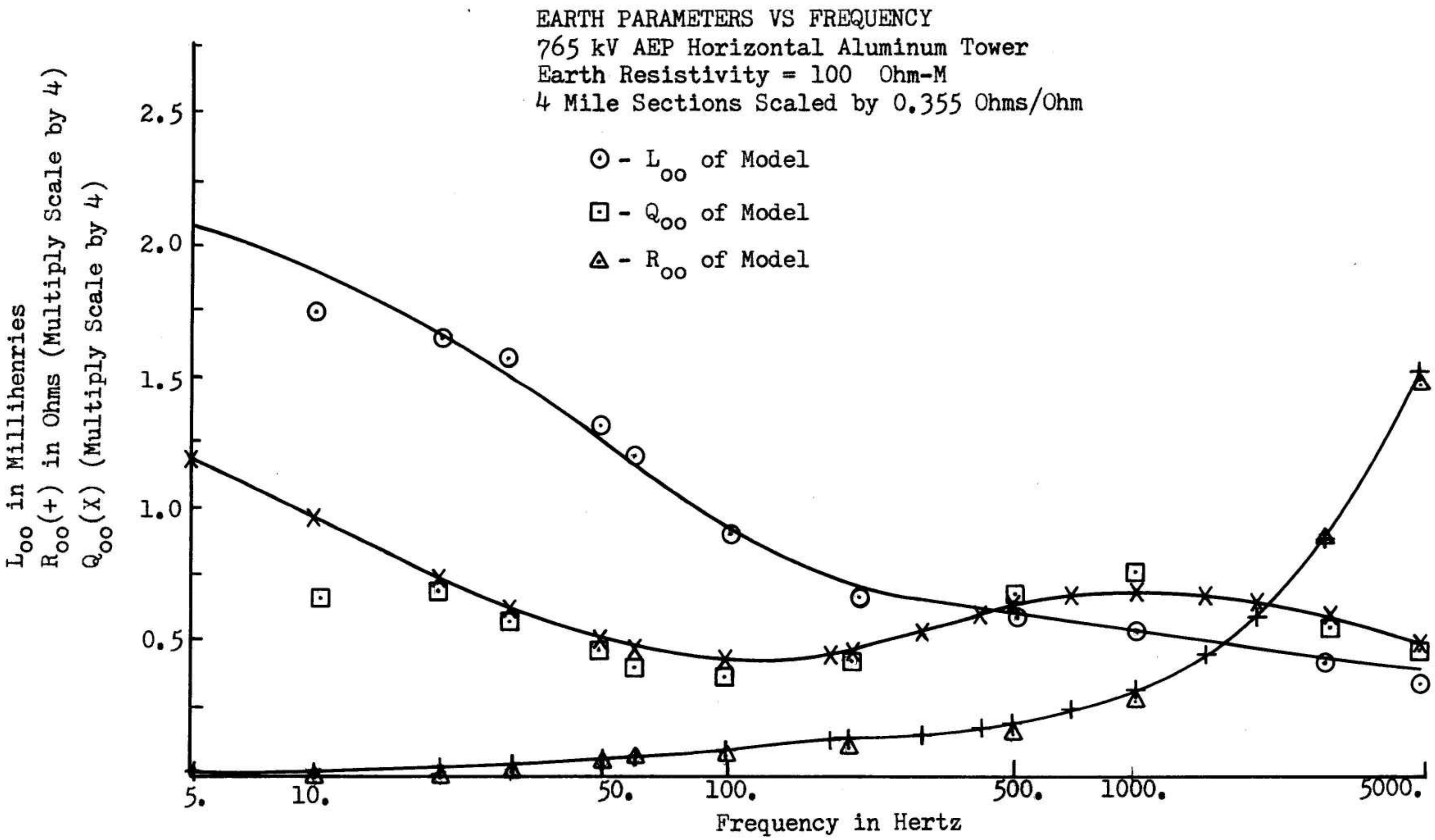

EARTH PARAMETERS VS FREQUENCY
765 kV AEP Horizontal Aluminum Tower
Earth Resistivity = 100 Ohm-M
4 Mile Sections Scaled by 0.355 Ohms/Ohm
⊙ - L_{oo} of Model
⊡ - Q_{oo} of Model
△ - R_{oo} of Model
L_{oo} in Millihenries
$R_{oo}(+)$ in Ohms (Multiply Scale by 4)
$Q_{oo}(X)$ (Multiply Scale by 4)
2.5
2.0
1.5
1.0
0.5
5.
10.
50.
100.
500.
1000.
5000.
Frequency in Hertz

Figure 6.3

EARTH PARAMETERS VS FREQUENCY
765 kV AEP Horizontal Aluminum Tower
Earth Resistivity = 1000 Ohm-M
4 Mile Sections Scaled by 0.355 Ohms/Ohm

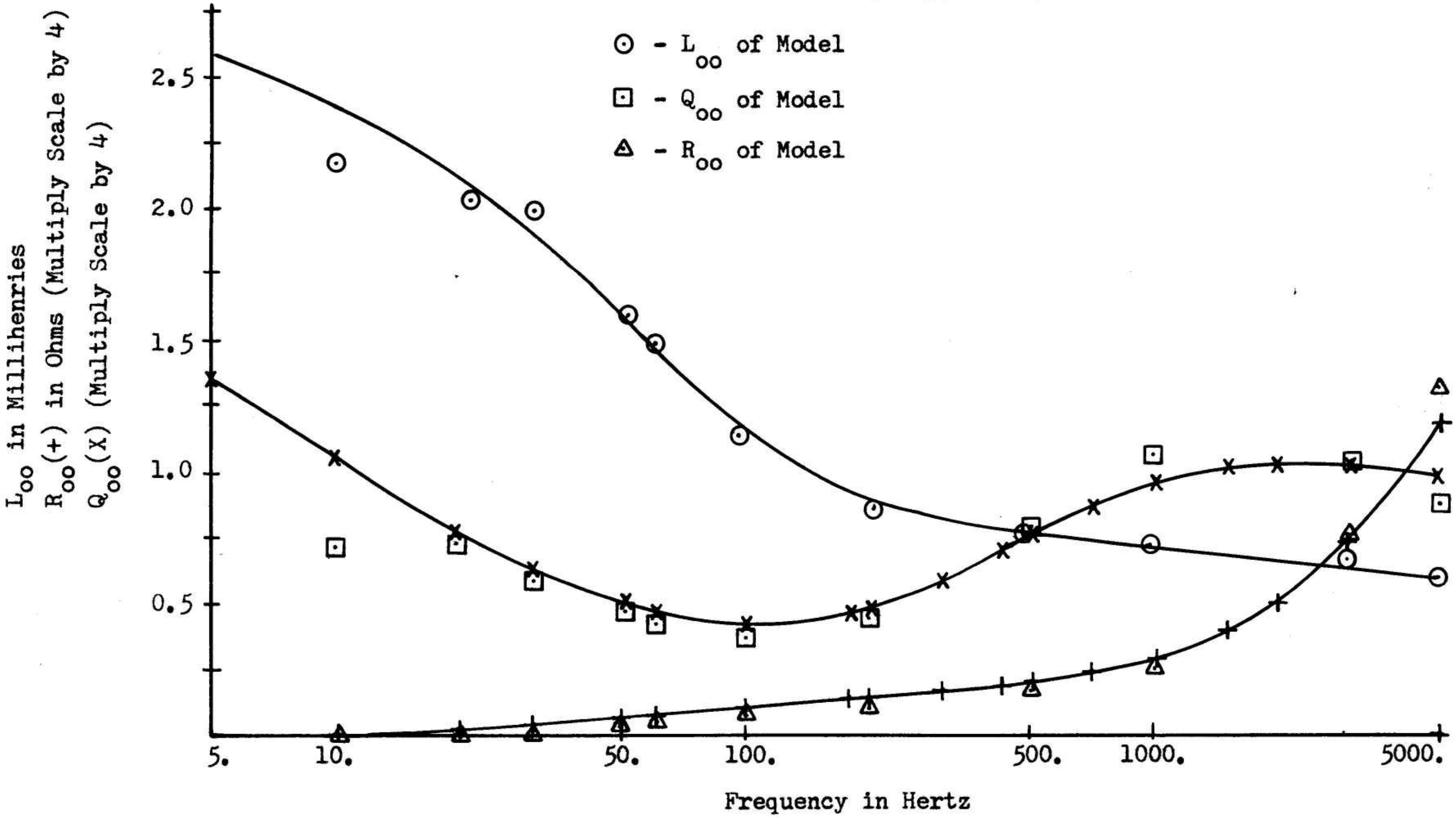

Figure 6.4

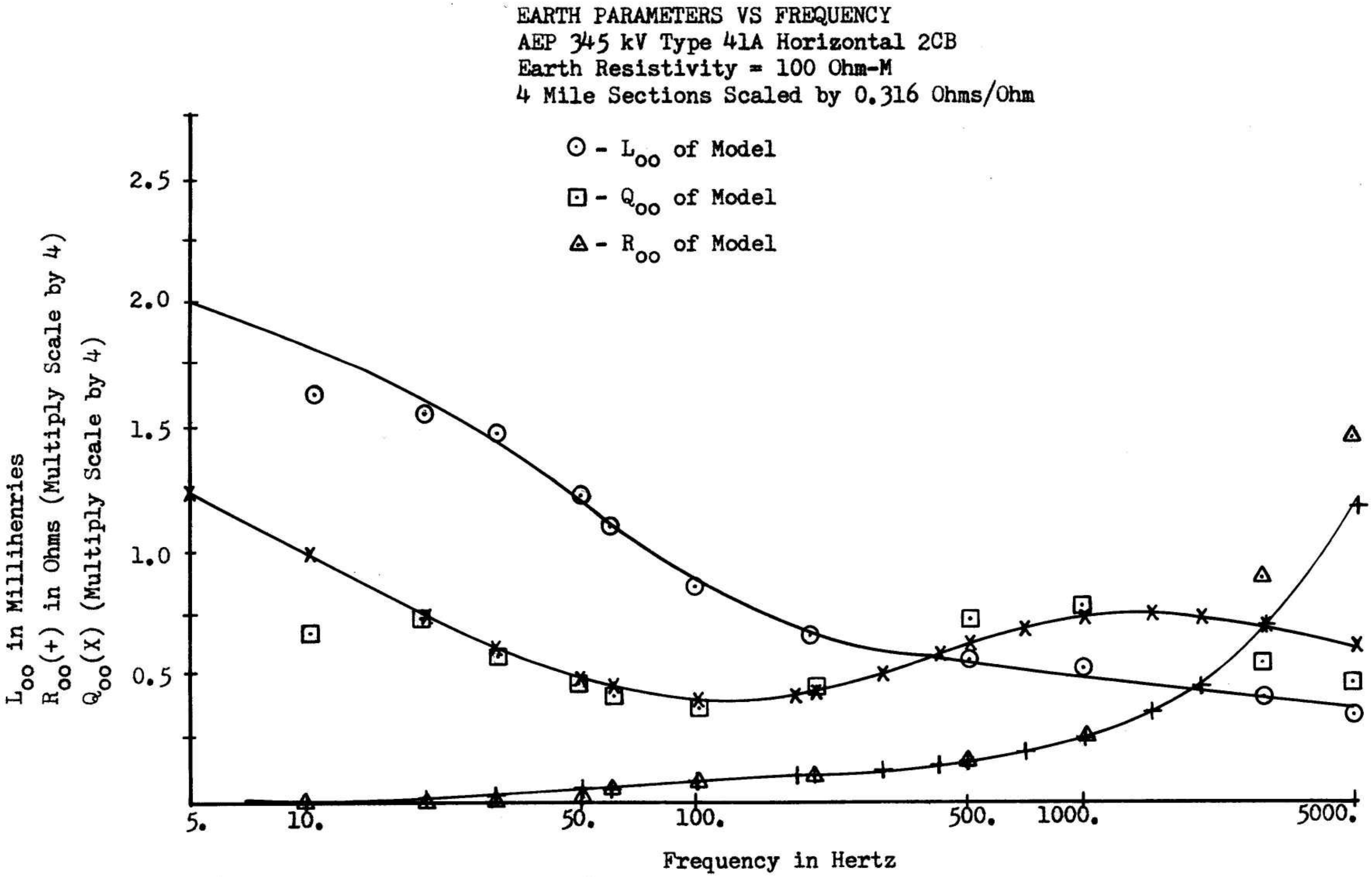
EARTH PARAMETERS VS FREQUENCY
AEP 345 kV Type 41A Horizontal 2CB
Earth Resistivity = 100 Ohm-M
4 Mile Sections Scaled by 0.316 Ohms/Ohm
- L_{oo} of Model
- Q_{oo} of Model
- R_{oo} of Model
L_{oo} in Millihenries
$R_{oo}(+)$ in Ohms (Multiply Scale by 4)
$Q_{oo}(X)$ (Multiply Scale by 4)
2.5
2.0
1.5
1.0
0.5
5.
10.
50.
100.
500.
1000.
5000.
Frequency in Hertz

Figure 6.5

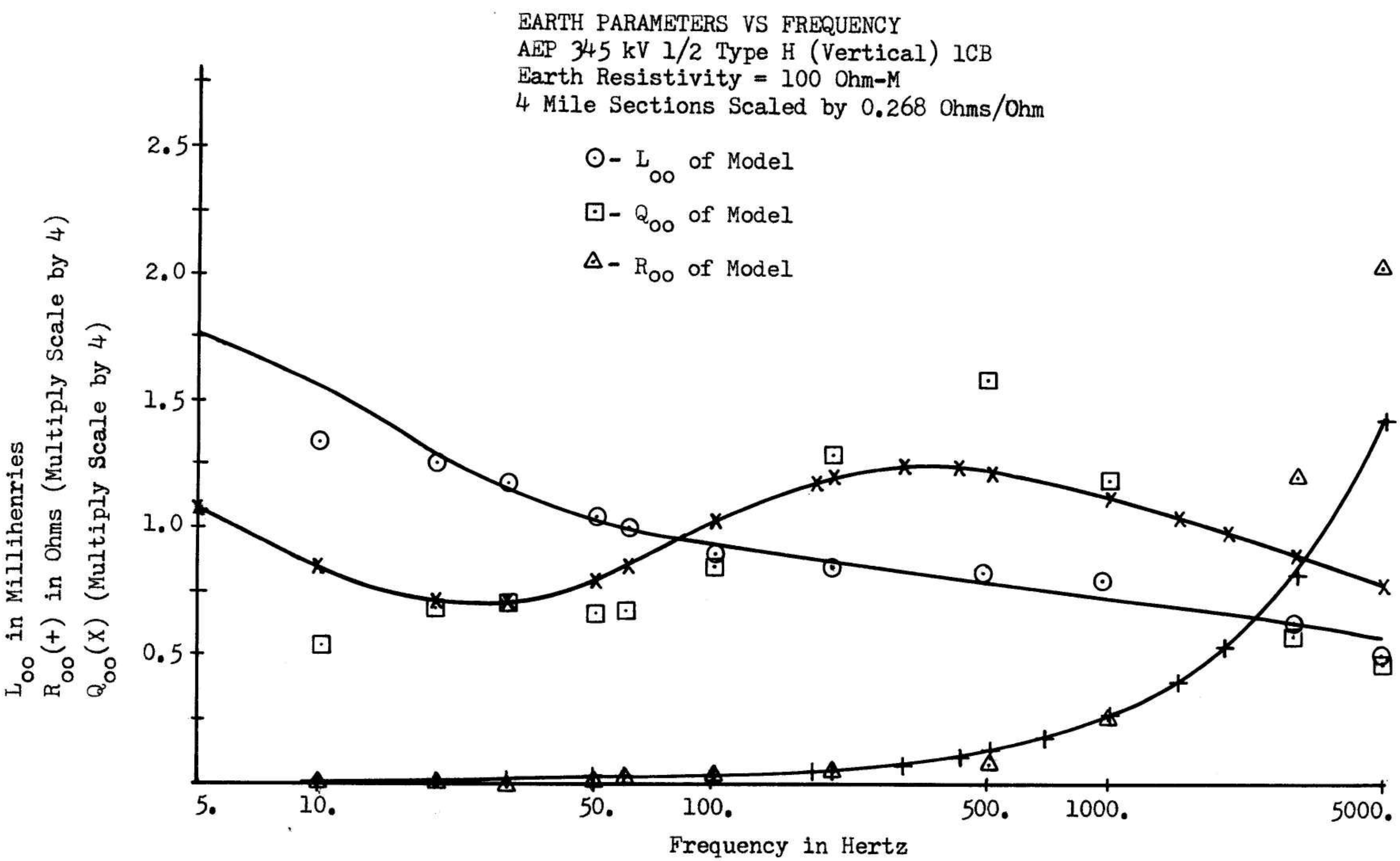
EARTH PARAMETERS VS FREQUENCY
AEP 345 kV 1/2 Type H (Vertical) 1CB
Earth Resistivity = 100 Ohm-M
4 Mile Sections Scaled by 0.268 Ohms/Ohm
⊙- L_{oo} of Model
⊡- Q_{oo} of Model
△- R_{oo} of Model
L_{oo} in Millihenries
$R_{oo}(+)$ in Ohms (Multiply Scale by 4)
$Q_{oo}(X)$ (Multiply Scale by 4)
2.5
2.0
1.5
1.0
0.5
5.
10.
50.
100.
500.
1000.
5000.
Frequency in Hertz

Figure 6.6

EARTH PARAMETERS VS FREQUENCY
AEP 345 kV 1/2 Type H (Vertical) 1CB
Earth Resistivity = 1000 Ohm-M
4 Mile Sections Scaled by 0.268 Ohms/Ohm

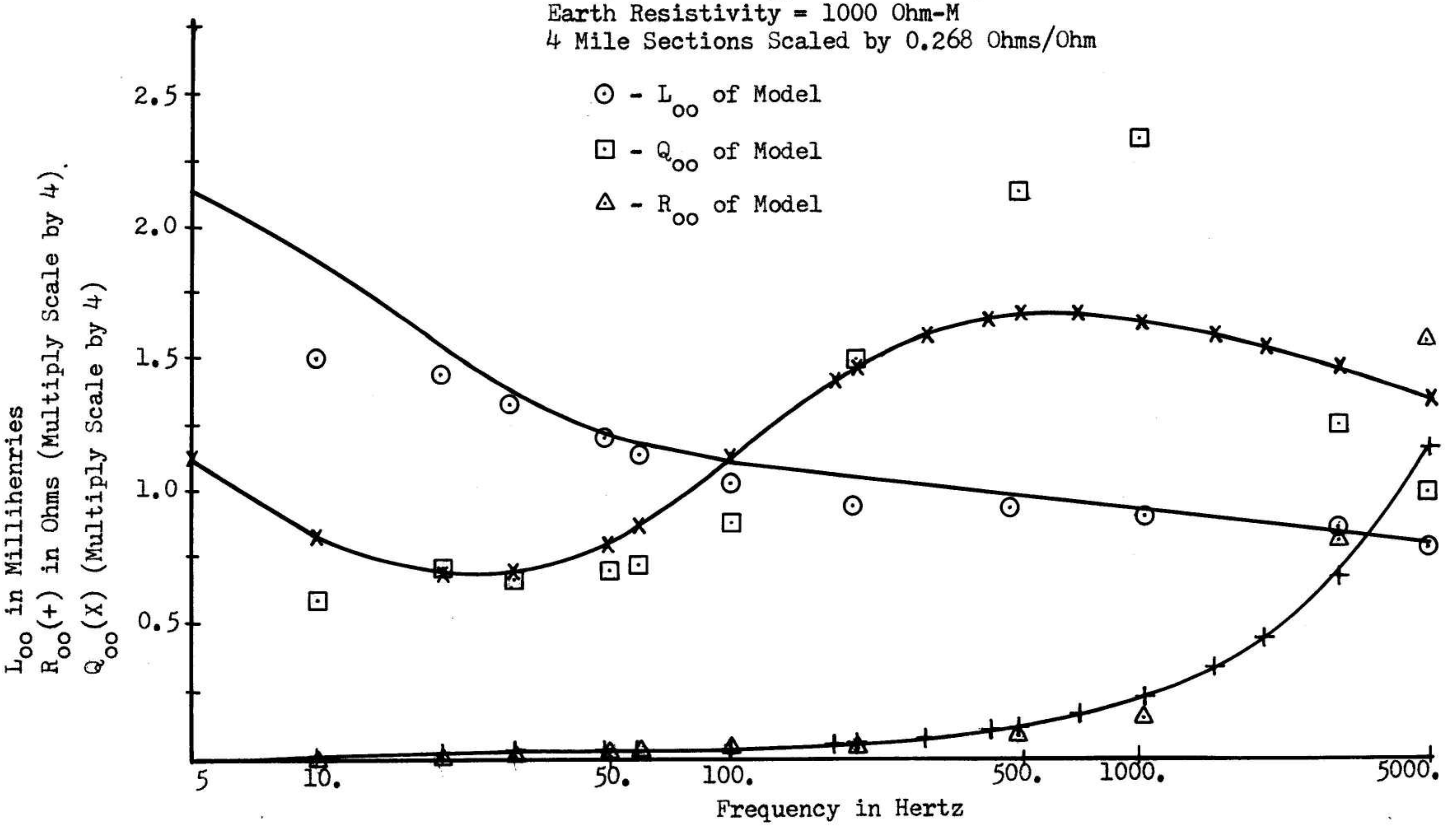

Figure 6.7

EARTH PARAMETERS VS FREQUENCY
AEP 345 kV 1/2 Type 39 2CB
Earth Resistivity = 100 Ohm-M
4 Mile Sections Scaled by 0.333 Ohms/Ohm

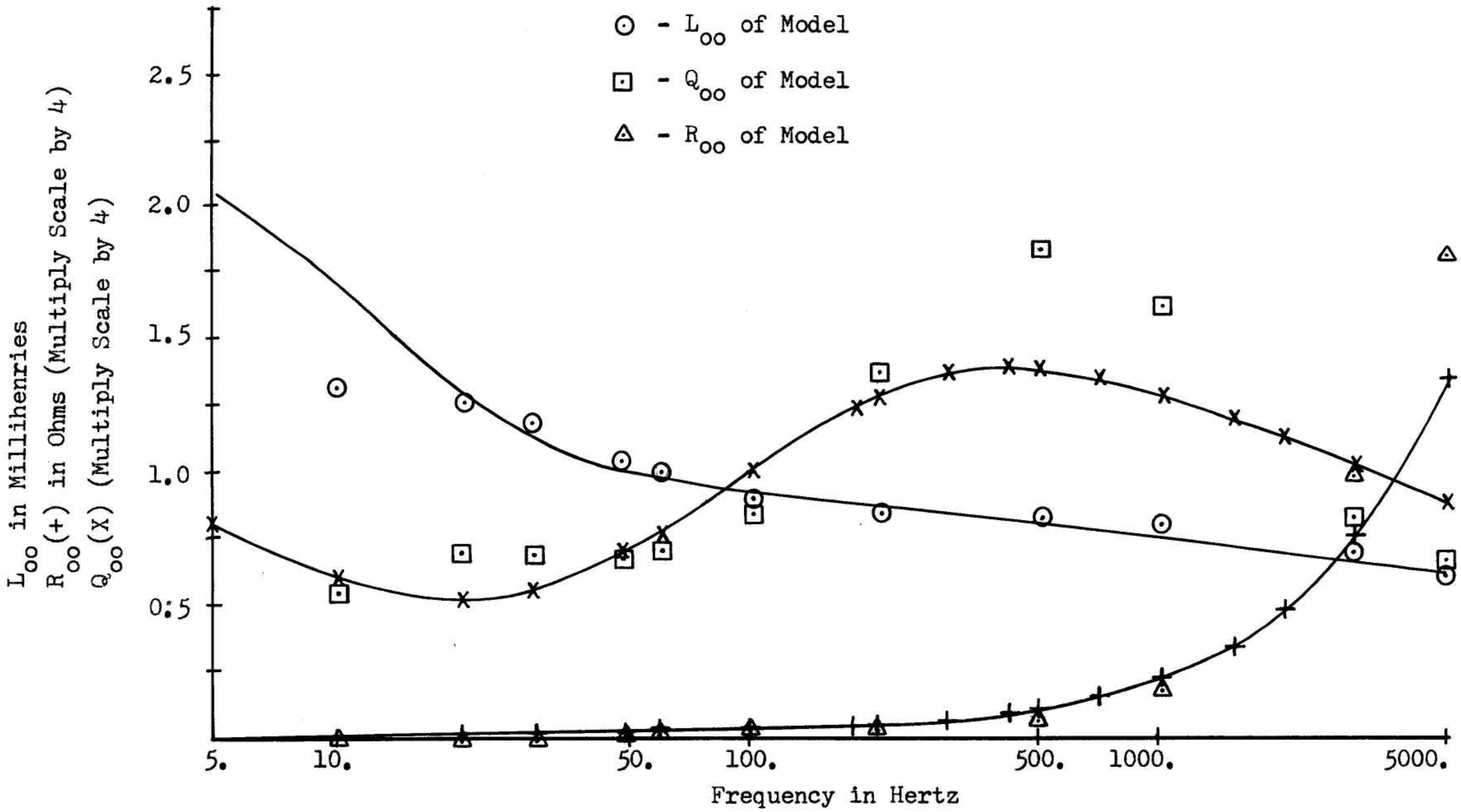

Figure 6.8

EARTH PARAMETERS VS FREQUENCY
AEP 345 kV 1/2 Type 39 2CB
Earth Resistivity = 1000. Ohm-M
4 Mile Sections Scaled by 0.333 Ohms/Ohm

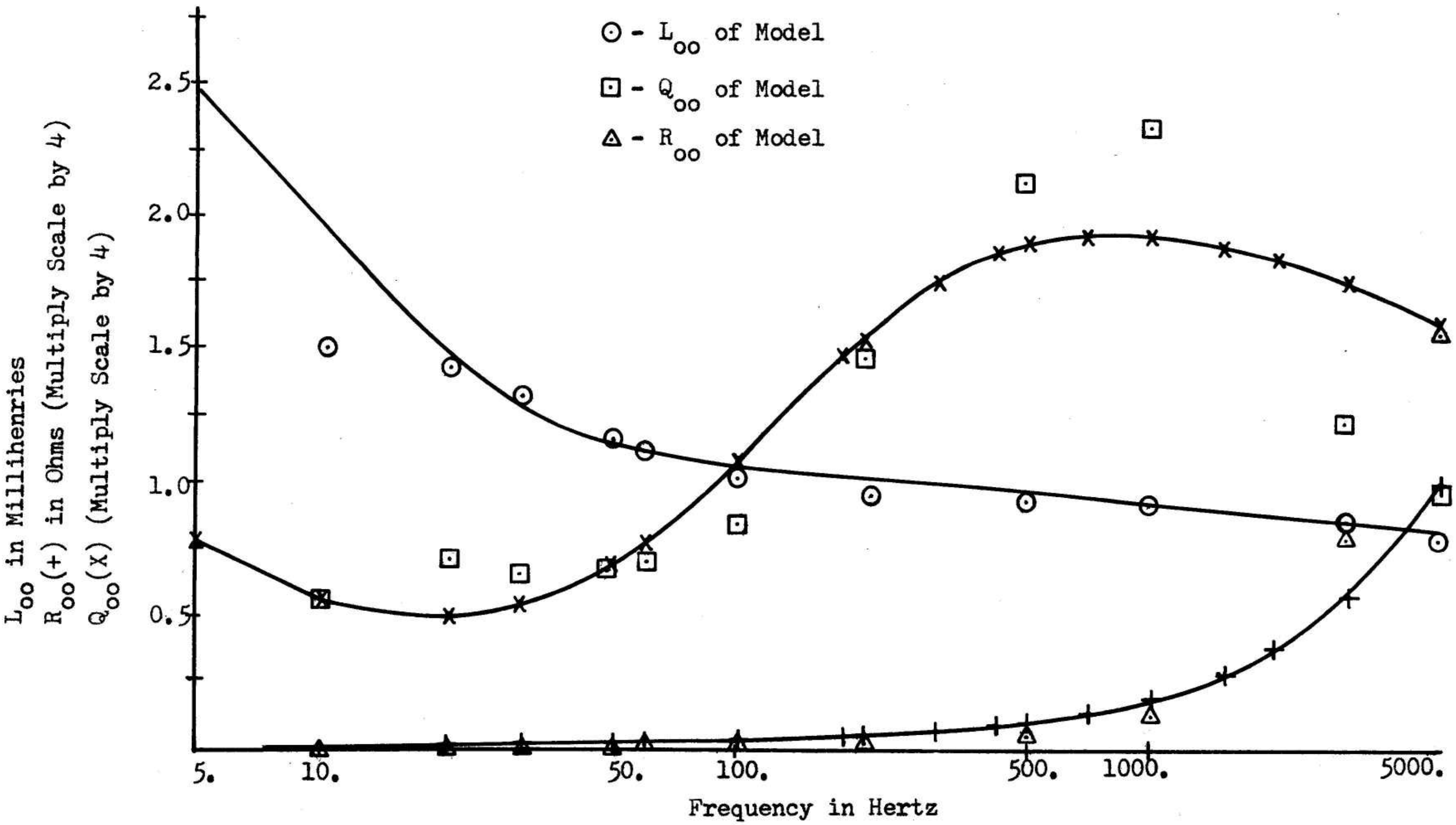

Figure 6.9

predicted from Chapter 4. However the error is not considered great enough to warrant going to a much more expensive coil design. The recommendations of Chapter 7 will discuss this point further.

Tables 6.3 through 6.9 give a tabulation of the results of the impedance vs frequency test for each of the coils with the various metallic disks in place. The measurements were made on the top tap, Tap 6, for each coil. By using the fractions given in Tables 5.1 and 5.2 and the program listed in Appendix C it should be possible to closely fit the Z_{oo} of almost any horizontal or vertical configuration transmission line. In these tables the R, L, and Q's at each frequency are listed to facilitate hand computations.

Table 6.10 tabulates the taps and disks required to fit the American Electric Power Company lines that were investigated during the course of this thesis.

Table 6.3

Impedance Parameters of the E Coil for a 4 Mile Section at Top Tap (Tap 6) with Copper Disks 1.0" Radius and 0.010" Thick

Frequency in Hertz	Current* in Amps	Voltage* in Volts	Shift** in Division	Resistance in Ohms	Inductance in Millihenries	Q
10	0.0578	0.0061	1.99	0.033	1.59	3.01
20	0.0578	0.0114	1.90	0.073	1.45	2.52
30	0.0578	0.0170	1.70	0.141	1.36	1.81
50	0.0578	0.0235	1.45	0.249	1.02	1.28
60	0.0578	0.0260	1.30	0.307	0.87	1.06
100	0.0578	0.0320	1.00	0.447	0.52	.73
200	0.0578	0.0378	.80	0.573	0.25	.55
500	0.0578	0.0440	.90	0.642	0.13	.63
1000	0.0578	0.0545	1.15	0.707	0.10	.88
3000	0.0578	0.1090	1.73	0.877	0.09	1.90
5000	0.0578	0.1610	1.85	1.10	0.08	2.31

*Current and Voltages are recorded in peak to peak values.
**One division is equivalent to 36 degrees.

Table 6.4

Impedance Parameters of the E Coil for a 4 Mile Section at Top Tap (Tap 6) with Copper Disks 1.5" Radius and 0.020" Thick

Frequency in Hertz	Current* in Amps	Voltage* in Volts	Shift** in Division	Resistance in Ohms	Inductance in Millihenries	Q
10	0.0578	0.0041	1.75	0.032	1.01	2.00
20	0.0578	0.0073	1.63	0.066	0.86	1.60
30	0.0578	0.0093	1.43	0.100	0.67	1.26
50	0.0578	0.0130	1.15	0.169	0.48	.89
60	0.0578	0.0135	1.09	0.182	0.39	.81
100	0.0578	0.0155	.90	0.226	0.23	.63
200	0.0578	0.0175	.90	0.256	0.13	.63
500	0.0578	0.0230	1.25	0.282	0.09	1.00
1000	0.0578	0.0345	1.70	0.288	0.08	1.80
3000	0.0578	0.0900	2.1	0.342	0.08	4.40
5000	0.0578	0.140	2.1	0.565	0.08	4.40

* Current and Voltages are recorded in peak to peak values.
**One division is equivalent to 36 degrees.

Table 6.5

Impedance Parameters vs Frequency for a 4 Mile Section, G Coil, Tap 6, Phosphorbronze Disk, 0.47" Radius and 0.005" Thick

Frequency in Hertz	Current* in Amps	Voltage* in Volts	Shift** in Division	Resistance in Ohms	Inductance in Millihenries	Q
10	0.060	0.0032	2.00	0.016	0.81	3.07
20	0.060	0.0064	2.25	0.017	0.84	6.30
30	0.060	0.0096	2.32	0.018	0.84	8.79
50	0.060	0.0160	2.32	0.030	0.84	8.79
60	0.060	0.0192	2.36	0.028	0.84	11.30
100	0.060	0.0320	2.39	0.044	0.85	12.10
200	0.060	0.064	2.33	0.113	0.84	9.31
500	0.060	0.156	2.15	0.567	0.81	4.47
1000	0.060	0.275	1.90	1.680	0.68	2.52
3000	0.060	0.540	1.50	5.290	0.39	1.37
5000	0.060	0.680	1.42	7.110	0.28	1.24

*Current and Voltages are recorded in peak to peak values.
**One division is equivalent to 36 degrees.

Table 6.6

Impedance Parameters vs Frequency for a 4 Mile Section, G Coil, Tap 6, Phosphorbronze Disk 0.35" Radius and 0.005" Thick

Frequency in Hertz	Current* in Amps	Voltage* in Volts	Shift** in Division	Resistance in Ohms	Inductance in Millihenries	Q
10	0.060	0.0033	2.01	0.017	0.85	3.14
20	0.060	0.0064	2.25	0.017	0.84	6.30
30	0.060	0.0097	2.32	0.018	0.85	8.79
50	0.060	0.0163	2.34	0.027	0.86	9.90
60	0.060	0.0194	2.35	0.030	0.85	10.50
100	0.060	0.0325	2.39	0.037	0.86	14.40
200	0.060	0.0650	2.38	0.082	0.86	13.20
500	0.060	0.160	2.26	0.400	0.84	6.57
1000	0.060	0.300	2.09	1.270	0.77	3.79
3000	0.060	0.700	1.65	5.930	0.53	1.69
5000	0.060	0.910	1.50	8.910	0.39	1.37

*Current and Voltage are recorded in peak to peak values.
**One division is equivalent to 36 degrees

Table 6.7

Impedance Parameters vs Frequency for a 4 Mile Section, G Coil, Tap 6, Phosphorbronze Disk 0.275" Radius and 0.005" Thick

Frequency in Hertz	Current* in Amps	Voltage* in Volts	Shift** in Division	Resistance in Ohms	Inductance in Millihenries	Q
10	0.060	0.0034	2.00	0.017	0.86	3.07
20	0.060	0.0066	2.25	0.017	0.86	6.30
30	0.060	0.0099	2.34	0.017	0.87	9.90
50	0.060	0.0165	2.35	0.026	0.87	10.50
60	0.060	0.0200	2.36	0.029	0.88	11.30
100	0.060	0.0330	2.40	0.035	0.87	15.80
200	0.060	0.0660	2.41	0.062	0.87	17.60
500	0.060	0.165	2.34	0.276	0.87	9.90
1000	0.060	0.320	2.20	0.999	0.83	5.23
3000	0.060	0.790	1.85	5.230	0.64	2.32
5000	0.060	1.090	1.70	8.750	0.51	1.81

* Current and Voltages are recorded in peak to peak values.
** One division is equivalent to 36 degrees.

Table 6.8

Impedance Parameters vs Frequency for a 4 Mile Section, G Coil, Tap 6, Phosphorbronze Disk 0.24" Radius and 0.005" Thick

Frequency in Hertz	Current* in Amps	Voltage* in Volts	Shift** in Division	Resistance in Ohms	Inductance in Millihenries	Q
10	0.060	0.0033	2.00	0.017	0.83	3.07
20	0.060	0.0065	2.25	0.017	0.85	6.30
30	0.060	0.0098	2.31	0.019	0.86	8.32
50	0.060	0.0162	2.37	0.022	0.86	12.10
60	0.060	0.0195	2.38	0.025	0.86	13.20
100	0.060	0.0325	2.40	0.034	0.86	15.8
200	0.060	0.0650	2.43	0.048	0.86	22.6
500	0.060	0.162	2.38	0.203	0.86	13.2
1000	0.060	0.320	2.30	0.669	0.84	7.90
3000	0.060	0.860	2.02	4.250	0.73	3.21
5000	0.060	1.270	1.90	7.790	0.63	2.52

*Current and Voltages are recorded in peak to peak values.
**One division is equivalent to 36 degrees.

Table 6.9

Impedance Parameters vs Frequency for a 4 Mile Section, G Coil, Tap 6, Phosphorbronze Disk 0.20" Radius and 0.005" Thick

Frequency in Hertz	Current* in Amps	Voltage* in Volts	Shift** in Division	Resistance in Ohms	Inductance in Millihenries	Q
10	0.060	0.0033	2.00	0.017	0.83	3.07
20	0.060	0.0065	2.25	0.017	0.85	6.30
30	0.060	0.0097	2.32	0.018	0.85	8.79
50	0.060	0.0162	2.39	0.019	0.86	14.40
60	0.060	0.0195	2.40	0.020	0.86	15.80
100	0.060	0.0325	2.41	0.031	0.86	17.60
200	0.060	0.0650	2.42	0.054	0.86	19.80
500	0.060	0.163	2.41	0.153	0.86	17.60
1000	0.060	0.320	2.38	0.402	0.85	13.20
3000	0.060	0.920	2.19	2.96	0.80	5.06
5000	0.060	1.410	2.10	5.84	0.72	3.89

*Current and Voltages are recorded in peak to peak values.
**One division is equivalent to 36 degrees.

Table 6.10

Tap and Disk Combinations Required to fit
American Electric Power Transmission Lines

AEP Line Designation	Voltage Level in KV	Earth-Resistivity in Ohm-meters: 10		100		1000	
		Tap	Disk*	Tap	Disk*	Tap	Disk*
H Special (vertical)	345	E-T1 G-T3	Cu 1.5"x.020" PhB .47"x.005"	E-T2 G-T5	Cu 1.5"x.020" PhB .275"x.005"	E-T3 G-T6	Cu 1.5"x.020" PhB .2"x.005"
½H Special (vertical)	345	E-T1 G-T3	Cu 1.5"x.020" PhB .47"x.005"	E-T2 G-T5	Cu 1.5"x.020" PhB .275"x.005"	E-T3 G-T6	Cu 1.5"x.020" PhB .2"x.005"
½Type 39 (vertical)	345	E-T2 G-T3	Cu 1.5"x.020" Phb .35"x.005"	E-T2 G-T5	Cu 1.5"x.020" PhB .24"x.005"	E-T3 G-T6	Cu 1.5"x.020" PhB .2"x.005"
41A (Horizontal)	345	E-T1 G-T1	Cu 1.0"x.010" PhB .47"x.005"	E-T4 G-T2	Cu 1.0"x.010" PhB .275"x.005"	E-T6 G-T3	Cu 1.0"x.010" PhB .2"x.005"
765 kV (Horizontal)	765	E-T1 G-T1	Cu 1.0"x.010" PhB .47"x.005"	E-T5 G-T2	Cu 1.0"x.010" PhB .275"x.005"	E-T6 G-T4	Cu 1.0"x.010" PhB .2"x.005"

*Disk designation is metal (Cu = Copper, PhB = Phosphorbronze)
Radius in inches and Thickness in inches.

CHAPTER 7

SUMMARY AND RECOMMENDATIONS

7.1 Summary

A method of designing the frequency dependent parameters for the earth return path in a transmission line model has been presented. The frequency dependence is achieved by using the diffusion phenomena which causes the frequency dependence of the actual transmission line earth impedance. By using this phenomena a continuous and smooth characteristic fit for the Z_{oo} earth impedance has been obtained from 20 to 5000 Hz for all transmission line configuration lines investigated.

To develop an appreciation for how the diffusion characteristic fits with the analysis of the earth return impedance a review of Carson's work is presented in Chapter 2. Also in Chapter 2 some of the approximations used by later researchers in particular Wagner and Evans have been presented and discussed relative to the frequency range being considered for this model.

Chapter 3 develops a detailed analysis for the frequency response of a long solenoid with a homogeneous conductive core. This analysis is extended to various attempts at modeling the Z_{oo} impedance of the transmission system. The first one was to use ferromagnetic material for the core of the long solenoid but it was found not to be feasible. A brief discussion as to why ferromagnetic material was not an acceptable core material was presented. By reviewing the long solenoid analysis in Appendix A,advantage was taken of the diffusion phenomena but by using a disk of highly conductive metal in the air gap of a finely laminated ferromagnetic yoke. It was found that this method of simulating the frequency dependent impedances was accurately predicted by the long solenoid approach. The long solenoid diffusion model did not match the earth impedance through the entire frequency range of interest. Thus a technique for combining two copper disk circuits was developed to give an exact fit for any configuration of EHV transmission lines.

The time constraints of the thesis did not allow for actually constructing a complete transmission line model. However, a detailed model of a 4 mile section of the transmission line was built and Chapter 5 demonstrates how this model was constructed. In Chapter 6 detailed verification tests on the 4 mile model are presented. The 8 mile pi sections required for the TLM are designed and should actually produce a better fit at the low frequencies since the resistance to reactance ratio will be better. Although a compromise was made on the vertical configuration in exactness of fit it was strictly a matter of physical and monetary consideration. Theoretically a vertical configuration could also be fit as accurately as the horizontal configuration if there were no bounds on the dimensions and the cost.

7.2 Recommendations

It is recommended initially only the design for the horizontal configuration lines be constructed. As stated in this thesis reasonable accuracy with a change in disk size can be obtained for the vertical configuration. However it is not clear how important this earth dependent representation is. It is therefore suggested that the first work toward deciding its importance be an investigation by another researcher into the relative effects of a frequency dependent earth representation versus the conventional linear representation of the earth path. A linear representation can be achieved by by-passing the E coil and gapping the G coils with non-metallic spacers. In this case external resistance will have to be added to achieve the correct 60 Hz Q.

A possible alteration on design of the G coil is also suggested. It was found that it was difficult to wind the G coil and maintain the tap accuracy required since so few turns were used in the overall coil. The difference of a half turn creates more than 5 percent error in some instances. This can be altered by going to a 10 mil thick disk and adding more turns to gain the same inductance level. This would alleviate the criticalness of turn tapping but it would increase the low frequency resistance of the G coil. It should be noted that the AC resistance of the coils becomes dominant very rapidly and therefore only a very slight loss in accuracy at the very low frequencies would result. Also increasing the effective air gap should significantly reduce the ampere-turn error cited in Chapter 6.

APPENDICES

APPENDIX A

MAGNETIC DIFFUSION IN A LONG METAL ROD

Consider a long solenoid where $R \ll 1$ as shown in Figure A.1. A continuous surface current around the solenoid is approximated by many turns of fine wire wrapped around the circumference of the rod. The tangential H field is then

$$H = \frac{NI}{\ell} \tag{A-1}$$

Since the rod is to be a highly conductive material the diffusion equation

$$\frac{1}{\mu\sigma} \nabla^2 B = \frac{\partial B}{\partial t} \tag{A-2}$$

must be applied to find the field distribution inside the solenoid. In cylindrical coordinates this becomes

$$\frac{\partial B}{\partial r^2} + \frac{1}{r}\frac{\partial B}{\partial r} - \mu\sigma\frac{\partial B}{\partial t} = 0 \tag{A-3}$$

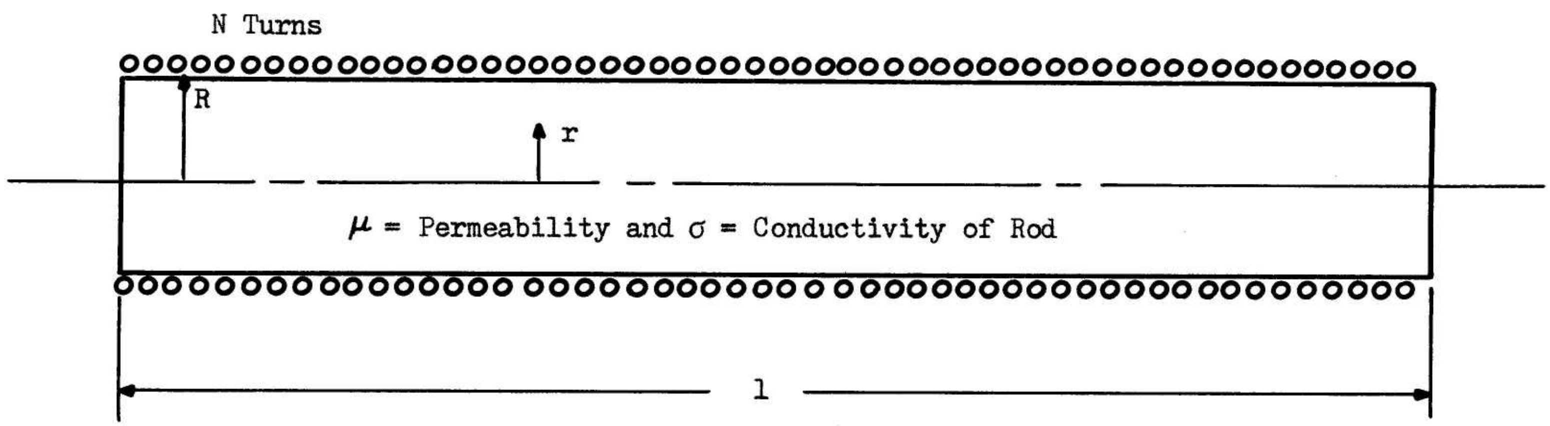

Long Solenoid Model of a Coil Wrapped on a Solid Metal Rod

Figure A.1

Since we are interested in frequency effects, let

$$B = \mathrm{Re}\left\{\hat{B}(r)\, e^{jwt}\right\} \tag{A-4}$$

which when substituted into (A-3) gives

$$\frac{\partial^2 \hat{B}(r)}{\partial r^2} + \frac{1}{r}\,\frac{\partial \hat{B}(r)}{\partial r} - j\,\omega\mu\sigma\,\hat{B}(r) = 0 \tag{A-5}$$

This is a form of Bessel's equation of zero order. Since the flux density must be finite at the center, we are only interested in solution of the first kind. Such a solution can be written as follows:[23,33,34]

$$\hat{B}(r) = C_1\left[\mathrm{ber}_0(r') + j\,\mathrm{bei}_0(r')\right] \tag{A-6}$$

where

$$r' = \sqrt{\omega\mu\sigma}\;r \tag{A-7}$$

To evaluate C_1 consider the boundary condition at $r = R$ described by equation (A-1). Since $B = \mu H$ then

$$\hat{B}(r) = \frac{\mu NI}{\ell}\;\frac{\left[\mathrm{ber}_0(r') + j\,\mathrm{bei}_0(r')\right]}{\mathrm{ber}\,(R)} \tag{A-8}$$

where

$$\mathrm{ber}(R) = \mathrm{ber}_0(\sqrt{\omega\mu\sigma}\, R) + j\, \mathrm{bei}_0(\sqrt{\omega\mu\sigma}\, R) \tag{A-9}$$

Now to compute the inductance of the solenoid, recall that the flux linkage is given by

$$\lambda = N \int B \cdot n\, da \tag{A-10}$$

therefore

$$\hat{\lambda} = N \int_0^R \int_0^{2\pi} \hat{B}(r)\, r\, d\theta\, dr \tag{A-11}$$

integrating with respect to theta

$$\hat{\lambda} = 2\pi N \int_0^R r\, \hat{B}(r)\, dr \tag{A-12}$$

substituting in equation (A-8)

$$\hat{\lambda} = \frac{2\pi\mu N^2 I}{\ell\, [\mathrm{ber}(R)]} \int_0^R r \left[\mathrm{ber}_0(r') + j\, \mathrm{bei}_0(r') \right] dr \tag{A-13}$$

changing the limits of integration to conform to equation (A-7) we get

$$\hat{\lambda} = \frac{2\pi N^2 I}{\left[\ell\omega\sigma \text{ ber}(R)\right]} \int_0^{R'} r'\left[\text{ber}_0(r') + j\,\text{bei}_0(r')\right] dr' \tag{A-14}$$

where

$$R' = \sqrt{\omega\mu\sigma}\ R \tag{A-15}$$

Integrating according to reference 34 equations 9.9.15 and 9.9.21 we get

$$\hat{\lambda} = \frac{\sqrt{2}\pi N^2 I\ R\sqrt{\omega\mu\sigma}}{\ell\omega\sigma\left[\text{ber}(R)\right]}\left[\text{bei}_1(R') - \text{ber}_1(R') - j\ \text{bei}_1(R') - j\,\text{ber}_1(R')\right] \tag{A-16}$$

conjugating and collecting terms

$$\hat{\lambda} = \left[\sqrt{\frac{2\mu}{\omega\sigma}}\right]\left[\frac{\pi N^2 I}{\ell}\right]\left[I\right]\left[\frac{U - jV}{|\text{ber}(R)|^2}\right] \tag{A-17}$$

where

$$U = \text{ber}_0(R')\left[\text{bei}_1(R') - \text{ber}_1(R')\right] - \text{bei}_0(R')\left[\text{bei}_1(R') + \text{ber}_1(R')\right] \tag{A-18}$$

$$V = \mathrm{bei}_0(R')\left[\mathrm{bei}_1(R') - \mathrm{ber}_1(R')\right] + \mathrm{ber}_0(R')\left[\mathrm{bei}_1(R') + \mathrm{ber}_1(R')\right] \qquad \text{(A-19)}$$

Since voltage across a coil is

$$v = \frac{d\lambda}{dt} = j\omega\hat{\lambda} \qquad \text{(A-20)}$$

and in circuit terms

$$v = r_s I + j\,\omega\, L I \qquad \text{(A-21)}$$

then the effective resistance of the coil must be

$$r_s = r_w + \left[\sqrt{\frac{2\mu}{\sigma}}\right]\left[\frac{\pi N^2 R}{\ell}\right]\left[\sqrt{\omega}\right]\left[\frac{V}{|\mathrm{ber}(R)|^2}\right] \qquad \text{(A-22)}$$

where r_w is the resistance of the winding. Similarly the inductance is given by

$$L = \left[\sqrt{\frac{2\mu}{\sigma}}\right]\left[\frac{\pi N^2 R}{\ell}\right]\left[\frac{1}{\sqrt{\omega}}\right]\left[\frac{U}{|\mathrm{ber}(R)|^2}\right] \qquad \text{(A-23)}$$

To make the U and V terms computationally simpler a transformation from reference 34, equation 9.9.16, can be used. By substituting the following

$$\mathrm{bei}_1(x) + \mathrm{ber}_1(x) = \sqrt{2}\,\mathrm{ber}_0'(x)$$
$$\mathrm{bei}_1(x) - \mathrm{ber}_1(x) = \sqrt{2}\,\mathrm{bei}_0'(x) \qquad \text{(A-24)}$$

where the primes indicate derivatives with respect to the argument x

into equations (A-18) and (A-19) we get

$$V' = \sqrt{2}\left[\mathrm{bei}_0(R')\,\mathrm{bei}_0'(R') + \mathrm{ber}_0(R')\,\mathrm{ber}_0'(R')\right] \qquad \text{(A-25)}$$

$$U' = \sqrt{2}\left[\mathrm{ber}_0(R')\,\mathrm{ber}_0'(R') - \mathrm{bei}_0(R')\,\mathrm{ber}_0'(R')\right] \qquad \text{(A-26)}$$

inserting these expressions into equations (A-22) and (A-23) and combining all the ber and bei functions into a single term we have

$$r_s = r_w + 2\left[\sqrt{\frac{\mu}{\sigma}}\right]\left[\frac{\pi N^2 R}{\ell}\right]\left[\sqrt{\omega}\right]\left[\bar{V}\right] \qquad \text{(A-27)}$$

$$L = 2\left[\sqrt{\frac{\mu}{\sigma}}\right]\left[\frac{\pi N^2 R}{\ell}\right]\left[\frac{1}{\sqrt{\omega}}\right]\left[\bar{U}\right] \qquad \text{(A-28)}$$

where

$$\bar{V} = \frac{\mathrm{bei}_0(R')\,\mathrm{bei}_0'(R') + \mathrm{ber}_0(R')\,\mathrm{ber}_0'(R')}{\left[\mathrm{ber}_0(R')\right]^2 + \left[\mathrm{bei}_0(R')\right]^2} \qquad \text{(A-29)}$$

$$\overline{U} = \frac{\mathrm{ber}_0(R')\,\mathrm{bei}_0'(R') - \mathrm{bei}_0(R')\,\mathrm{ber}_0'(R')}{\left[\mathrm{ber}_0(R')\right]^2 + \left[\mathrm{bei}_0(R')\right]^2} \qquad \text{(A-30)}$$

APPENDIX B

```
C  ***  FEERO SPECIAL BESSEL FUNCTION FOR EVALUATING NON-LINEAR INDUCTORS
C         THIS PROGRAM COMPUTES VARIOUS COMBINATIONS OF A DIFFUSION CONTROLLED
C         INDUCTOR IN SERIES WITH A LINEAR INDUCTOR.
C         THE ARGUMENT OF BESSEL MODIFIERS OF BOTH THE INDUCTANCE AND THE
C         RESISTANCE IS VARIED THRU A RANGE WHICH SEEMS LIKELY TO GIVE THE
C         TRANSMISSION LINE CHARACTERISTIC DESIRED.  THE COEFFICIENT OF THE
C         INDUCTANCE BESSEL MODIFIER IS ADJUSTED TO GIVE 1.16 MH AT 60 HZ
C         WHEN COMBINED WITH THE LINEAR INDUCTANCE.
C         THE RESULTANT R,L, AND Q ARE PRINTED AND PLOTTED
C
C         EL = COMBINED INDUCTANCE
C         R  = COMBINED RESISTANCE
C         Q  = COMBINED QUALITY FACTOR
C         F  = FREQUENCY IN HZ
C         FL = LOG TO THE BASE 10 OF THE FREQUENCY
C         RP = THE ARGUMENT OF THE BESSEL MODIFIERS AT 60 HZ
C         ELL= THE LINEAR INDUCTANCE
C         ELC= THE INDUCTANCE COEFFICIENT
C  ****
      DIMENSION EL(22),R(22),Q(22),F(22),FL(22)
      DATA F/1.,2.,5.,7.,10.,15.,20.,30.,50.,60.,80.,100.,150.,180.,
     1200.,300.,500.,700.,1000.,1800.,3000.,5000./
      DO 5 I=1,22
      FL(I) = ALOG(F(I))/2.3
 5    CONTINUE
C          RWIRE = .012 OHMS FOR 10 FT OF NO.10 WIRE
      RWIRE = 0.012 + .012
      ELL = 0.0
      DO 1000 IJ = 1,5
      ELL = ELL + .1E-03
      RP = 2.401
```

```
      DO 1000 IK = 1,7
      RP = RP + .3
      WRITE (3,9009)RP
 9009 FORMAT (5HO****,' 60 HZ VALUE OF R PRIME = ',F5.2)
      RC=RP/SQRT(2.3*3.1416*60.)
      CALL BER(RP,BERA)
      CALL BEI(RP,BEIA)
      CALL BERP(RP,BERPA)
      CALL BEIP(RP,BEIPA)
      BD=BERA**2+BEIA**2
      BL60=(BERA*BEIPA-BEIA*BERPA)/BD
      ELADJ=1.16E-03-ELL
      ELC=(ELADJ*SQRT(2.*3.1416*60.))/BL60
      DO 50 J=1,22
      W=2.*3.1416*F(J)
      RPP=RC*SQRT(W)
      IF (RPP-30.)20,20,30
   20 CALL BER(RPP,BERA)
      CALL BEI(RPP,BEIA)
      CALL BERP(RPP,BERPA)
      CALL BEIP(RPP,BEIPA)
      BD = BERA**2 + BEIA**2
      BL = (BERA*BEIPA-BEIA*BERPA)/BD
      GO TO 40
   30 BL = .707
      BR = .707
      GO TO 45
   40 BR = (BEIA*BEIPA + BERA*BERPA)/BD
   45 EL(J) = ELC*(1./SQRT(W))*BL + ELL
      R(J) = ELC*SQRT(W)*BR + RWIRE
      Q(J) = W*EL(J)/R(J)
```

```
      WRITE (3,9010)F(J),R(J),Q(J),EL(J)
9010  FORMAT(4H F=,E10.3,4H R=,E10.3,4H Q=,E10.3,5H EL=,E10.3 )
50    CONTINUE
7000  FORMAT (' LOO IN MILLIHENRIES ')
7001  FORMAT('AND')
7002  FORMAT('.5 ROO(+) IN OHMS AND .5QOO(X)')
7003  FORMAT(' FREQUENCY IN HZ')
7010  FORMAT(F3.1)
7011  FORMAT(F6.0)
7020  FORMAT ('R PRIME AT 60 HZ = ',F4.1)
      CALL SCALF ( 2.5,2.5,0.,0.)
      CALL FGRID ( 0,0.,0.,1.,4)
      CALL FGRID (1,0.,0.,.2,15)
      CALL FCHAR (-.45,.5,.2,.2,1.57)
      WRITE (7,7000)
      CALLFCHAR(-.3,1.3,.2,.2,1.57)
      WRITE (7,7001)
      CALL FCHAR(-.15,.2,.2,.2,1.57)
      WRITE(7,7002)
      CALL FCHAR (1.5,-.3,.2,.2,.0)
      WRITE (7,7003)
      Y =.201
      DO 60 I = 1,15
      CALL FCHAR (-.14,Y,.1,.1,0.)
      WRITE(7,7010)Y
      Y = Y + .2
60    CONTINUE
      X = -.15
      XX = 1.0
      DO 70 I =1,5
      CALL FCHAR(X,-.1,.1,.1,0.)
      WRITE (7,7011)XX
      X=X+1.
```

```
      XX = 10.*XX
 70   CONTINUE
      CALL FCHAR(1.,3.,.2,.2,.0)
      WRITE (7,7020)RP
C        TO PLOT L IN MILLIHENRIES
      CALL FPLOT(-2,0.,0.)
      DO 200 I=1,22
      ELM = 1000.*EL(I)
      CALL FPLOT(0,FL(I),ELM)
 200  CONTINUE
C        POINT(0) = ROO
      CALL FPLOT(+1,0.,0.)
      CALLSCALF (2.5,1.25,0.,0.)
      CALL FPLOT(+2,0.,0.)
      DO 210 I=1,22
      CALL FPLOT(0,FL(I),R(I))
      CALL POINT (0)
 210  CONTINUE
C        POINT(1) = QOO
      CALL FPLOT(+1,0.,0.)
      CALL FPLOT(+2,0.,0.)
      DO 220 I=1,22
      CALL FPLOT(0,FL(I),Q(I))
      CALL POINT (1)
 220  CONTINUE
      CALL FPLOT (+1,5.5,0.)
 1000 CONTINUE
      CALL EXIT
      END
```

```
C         SUBROUTINE FOR CALCULATING THE BER FUNCTION ZERO ORDER
      SUBROUTINE BER(X,BERX)
      TERM=1.
      BERX=1.
      TOP=(.25*X**2)**2
      B=2.
 1    BOT=(B*(B-1.))**2
      TERM=-(TOP/BOT)*TERM
      BERX=BERX+TERM
      B=B+2.0
      TEST = ABS( TERM/BERX )
      IF ( TEST - .0001)2,2,1
 2    RETURN
      END
C         SUBROUTINE FOR CALCULATING THE BEI FUNCTION ZERO ORDER
      SUBROUTINE BEI(X,BEIX)
      TERM=.25*X**2
      BEIX=.25*X**2
      B=3.0
      TOP=(.25*X**2)**2
 1    BOT=(B*(B-1.))**2
      TERM=-(TOP/BOT)*TERM
      BEIX=BEIX+TERM
      B=B+2.0
      TEST = ABS( TERM/BEIX )
      IF (TEST - .0001)2,2,1
 2    RETURN
      END
```

```
C          SUBROUTINE FOR CALCULATING THE DERIVATIVE OF THE BER FUNCTION ZERO ORDER
       SUBROUTINE BERP(X,BERPX)
       TERM=-(.25*X**2)*X/4.
       BERPX=TERM
       B=4.0
 1     TOP=(B/(B-2.))*(.25*X**2)**2
       BOT=(B*(B-1.))**2
       TERM=-(TOP/BOT)*TERM
       BERPX=BERPX+TERM
       B=B+2.0
       TEST = ABS( TERM/BERPX )
       IF ( TEST - .0001)2,2,1
 2     RETURN
       END
C          SUBROUTINE FOR CALCULATING THE DERIVATIVE OF THE BEI FUNCTION ZERO ORDER
       SUBROUTINE BEIP(X,BEIPX)
       TERM=X/2.
       BEIPX=X/2.
       B=3.0
 1     TOP=(B/(B-2.))*(.25*X**2)**2
       BOT=(B*(B-1.))**2
       TERM=-(TOP/BOT)*TERM
       BEIPX=BEIPX+TERM
       B=B+2.0
       TEST = ABS( TERM/BEIPX )
       IF ( TEST - .0001)2,2,1
 2     RETURN
       END
```

APPENDIX C

```
** FEERO TEST DATA CURVE ADJUSTING R L Q VS F
C        ***DEFINITION OF TERMS***
C          F1 = FREQUENCY COIL #1
C          F2 = FREQUENCY COIL #2
C          CR1= CURRENT COIL #1
C          CR2= CURRENT COIL #2
C          VL1= VOLTAGE COIL #1
C          VL2= VOLTAGE COIL #2
C          A1 = ANGLE,READ IN AS DIVISIONS,PRINTED OUT AS DEGREES, COIL #1
C          A2 = ANGLE,READ IN AS DIVISIONS,PRINTED OUT AS DEGREES, COIL #2
C          Z1 = IMPEDANCE OF COIL #1
C          Z2 = IMPEDANCE OF COIL #2
C          R1 = RESISTANCE OF COIL #1
C          R2 = RESISTANCE OF COIL #2
C          X1 = REACTANCE OF COIL #1
C          X2 = REACTANCE OF COIL #2
C          L1 = INDUCTANCE OF COIL #1
C          L2 = INDUCTANCE OF COIL #2
C          Q1 = QUALITY FACTOR OF COIL #1
C          Q2 = QUALITY FACTOR OF COIL #2
C          L  = INDUCTANCE OF THE COMBINATION OF COIL #1 AND #2
C          R  = RESISTANCE OF THE COMBINATION OF COIL #1 AND #2
C          Q  = QUALITY FACTOR OF THE COMBINATION OF COIL #1 AND #2
      REAL L1(15),L2(15),LA,L11(15)
      DIMENSION F1(15),F2(15),CR1(15),CR2(15),VL1(15),VL2(15),A1(15),
     1 A2(15),Z1(15),Z2(15),R1(15),R2(15),X1(15),X2(15),R(15),Q(15),
     1 Q1(15),Q2(15),R11(15)
C          READ TITLE CARD OF FIRST COIL
      READ(2,9000)
 9000 FORMAT ('
     1                    ')
```

```
C         READ IN COUNT OF DATA POINTS OF FIRST COIL AND TAP MULTIPLE
      READ (2,9002)NDAT1,XM1
 9002 FORMAT (I5,F6.4)
C         READ IN DATA POINTS OF FIRST COIL
      READ(2,9004)(F1(I),CR1(I),VL1(I),A1(I),I=1,NDAT1)
 9004 FORMAT (4E10.4)
 9007 FORMAT (////' ')
C         READ TITLE CARD OF SECOND COIL
      READ (2,9010)
 9010 FORMAT ('
     1                          ')
C         READ COUNT OF DATA POINTS OF SECOND COIL AND TAP MULTIPLE
      READ (2,9002)NDAT2,XM2
C         READ DATA POINTS OF SECOND COIL
      READ (2,9004)(F2(I),CR2(I),VL2(I),A2(I),I=1,NDAT2)
C         CALCULATE IMPEDANCE PARAMETERS OF FIRST COIL
      DO 10 I=1,NDAT1
      Z1(I) = VL1(I)/CR1(I)
      A1(I) = A1(I)*36.
      A = A1(I)/57.3
      R1(I) - Z1(I)*COS(A)
      X1(I) = Z1(I)*SIN(A)
      L1(I) = X1(I)/(F1(I)*6.28)
      Q1(I) = X1(I)/R1(I)
 10   CONTINUE
C         CALCULATE IMPEDANCE PARAMETERS OF SECOND COIL
      DO 20 I = 1,NDAT2
      Z2(I) = VL2(I)/CR2(I)
      A2(I) = A2(I)*36.
      A = A2(I)/57.3
      R2(I) = Z2(I)*COS(A)
      X2(I) = Z2(I)*SIN(A)
      L2(I) = X2(I)/(F2(I)*6.28)
      Q2(I) = X2(I)/R2(I)
```

```
 20     CONTINUE
        WRITE (3,9000)
        WRITE (3,9002)NDAT1,CODE1
        WRITE (3,9003)
 9003   FORMAT ('      FREQ      VOLTAGE    CURRENT    ANGLE         ZX          RX
      1         XX          LX          QX')
        WRITE (3,9006)(F1(I),VL1(I),CR1(I),A1(I),Z1(I),R1(I),X1(I),L1(I),Q
      11(I),I=1,NDAT1)
 9006   FORMAT (9E10.3)
        WRITE (3,9007)
        WRITE (3,9010)
        WRITE (3,9002)NDAT2,CODE2
        WRITE (3,9003)
        WRITE (3,9006)(F2(I),VL2(I),CR2(I),A2(I),Z2(I),R2(I),X2(I),L2(I),Q
      12(I),I=1,NDAT2)
C          ADJUST FIRST COIL TO XM1
 30     RDC1 = .015*SQRT(XM1)+.015
        DO 34 I=1,NDAT1
        R11(I) = XM1*(R1(I)-.030) + RDC1
        L11(I) = XM1*L1(I)
 34     CONTINUE
C          ADJUST SECOND COIL TO XM2 AND COMBINE RESULTS
 40     RDC2 = R2(1)*SQRT(XM2)
        WRITE (3,9021)XM1,XM2
 9021   FORMAT (///'    FREQ      L          R          Q          XM1=',F6.3,5H
      1 XM2=,F6.3)
        K = 0
        DO 60 J=1,NDAT2
        K = K + 1
        IF (F1(K)-F2(J))50,45,50
 50     K = K -1
        GO TO 60
```

```
45     RA = XM2*(R2(J)-R2(1)) + RDC2
       LA = XM2*L2(J)
       L(J) = L11(K) + LA
       R(J) = R11(K) + RA
       Q(J) = (L(J)*6.28*F2(J))/R(J)
       WRITE (3,9006) F2(J),L(J),R(J),Q(J)
60     CONTINUE
100    CALL EXIT
       END
```

LIST OF REFERENCES

In Order Cited:

1. Dillard, J.K., Clayton, J.M.,Jr., and Kilar, L.A., Controlling Switching Surges on 1100 kV Transmission Systems, IEEE Trans. P.A.S. 89, November-December, 1970, p.p. 1752-1762.

2. Bush, V., The Differential Analyzer, A New Machine for Solving Differential Equations, Journal of the Franklin Institute, 212, No. 4, October, 1931, p.p. 447-488.

3. Evans, R.D. and Monteith, A.C., System Recovery Voltage Determination by Analytical and A.C. Calculating Board Methods, AIEE Trans. 56, 1937, p.p. 695-705.

4. Peterson, H.A., An Electric Circuit Transient Analyzer, General Electric Review, September, 1939, p.p. 394-400.

5. Kuehni, H.P., and Peterson, H.A., A New Differential Analyzer, AIEE Trans. 63, 1944, p.p. 221-228.

6. Harder, E.L. and McCann, G.D., A Large Scale General Purpose Electric Analog Computer, AIEE Trans. Vol. 67, 1948, p.p. 664-673.

7. Wilson, G.L. and Bosack, D.J., Effects of Non-Transposition on Steady-State Overvoltages on EHV Transmission Lines, Report No. 5 of the Power System Engineering Group, Department of Electrical Engineering, M.I.T., Cambridge, Mass.

8. Central Station Engineers of Westinghouse Electric Corporation, Electrical Transmission and Distribution Reference Book, Westinghouse Electric Corporation, East Pittsburgh, Pa. 1964.

9. Carson, J.R., Wave Propagation in Overhead Wires with Ground Return, Bell System Technical Journal, Vol. 5, 1926, p.p. 539-554.

10. Wagner, C.F. and Evans, R.D., Symmetrical Components, McGraw-Hill Book Company, 1933.

11. Lewis, W.A. and Tuttle, P.D., The Resistance and Reactance of Aluminum Conductor Steel Reinforced, Trans. AIEE, Vol. 77, pt. III, 1958, p.p. 1189-1215.

12. Hylten-Cavallius, N. and Gjerlov, P., Distortion of Traveling Waves in High-Voltage Power Lines, ASEA Research 2, 1959, p.p. 147-180.

13. Hedman, D.E., Propagation on Overhead Transmission Lines, Pt.II: Earth Conduction Effects and Practical Results, IEEE Trans. P.A.S. 84, March, 1965, p.p. 200-205.

14. Vokcker, O., Internal Documents of C.I.G.R.E. Working Group 13.5, Working Group 13.5 C.I.G.R.E., 1968.

15. Clerici, A. and Taschini, A., Influence on Switching Surges of the Switched Line Zero Sequence Impedance, IEEE Trans. P.A.S. Vol. 90, February, 1970, p.p. 1327-1334.

16. Thoren, H.B. and Carlson, K.L., A Digital Computer Program for the Calculation of Switching and Lightning Surges on Power Systems, IEEE Trans. P.A.S. Vol. 89, February,1970, p.p. 212-218.

17. Budner, A., Introduction of Frequency-Dependent Line Parameters into an Electromagnetic Transients Program, IEEE Trans. P.A.S. Vol. 89, January, 1970, p.p. 88-97.

18. Robert, J.A., and Tran-Dinh, K., New Digital Simulation for Ground-Mode Switching Surge Response of EHV Transmission Systems, Vol. P.A.S. 88, May, 1969, p.p. 587-603.

19. Brown, G.W., Feero, W.E., Juves,J.A. and Long, R.W., Transmission Line Response to a Surge with Earth Return, IEEE Trans. P.A.S. Vol.90, May/June, 1971, p.p. 1112-1121.

20. Russell, W.A., Frequency Dependence of Propagation on a Three Phase Transmission Line, Master of Science Thesis, University of Maryland, 1971.

21. Schmidt, K.A. and Wilson, G.L., Design of a Non-Transposed Power Transmission Line Model, Electric Power Systems Engineering Laboratory, Report No. 29, May, 1971, M.I.T., Cambridge, Mass.

22. Bewley, L.V., Traveling Waves on Transmission Lines, Dover Publications, 2nd Edition, 1963.

23. Stevenson, W.D.,Jr., Elements of Power System Analysis, McGraw-Hill Book Company, 1955.

24. Sunde, E.D., Earth Conduction Effects in Transmission Systems, Dover Publications, Inc., New York, N.Y., 1949.

25. Wilson, G.L., Electric Power Systems Laboratory Line and Model Parameters Program, M.I.T., 1969. An unpublished program written for the Laboratory and maintained in Professor Wilson's custody.

26. Young, F.J., Ferromagnetic Shielding Related to the Physical Properties of Iron, IEEE Electromagnetic Compatability Symposium Rec., 1968, p.p. 88-95.

27. Ferber, R.R. and Young, F.J., Shielding Electromagnetic Pulses by Use of Magnetic Materials, 1969 IEEE Electromagnetic Compatability Symposium Rec., p.p. 73-79.

28. Young, F.J. and English, W.J., Flux Distribution in a Linear Magnetic Shield, IEEE Trans. Vol. EMC-12, No.3, August, 1970.

29. M.I.T. Electrical Engineering Staff, Magnetic Circuits and Transformers, John Wiley and Sons, Inc., New York, 1943.

30. Arnold Engineering Co., Arnold Silectron Cores, Arnold Engineering Co. Bulletin S.C.-107B, Merengo, Illinois.

31. Ferroxcube Corporation, Ferroxcube Linear Ferrite Materials and Components, Ferroxcube Corporation, Saugerties, N.Y.

32. Indiana General Company, Ferramic Materials and Components, Indiana General Catalog No. 107, Keasbey, New Jersey.

33. Melcher, J.R. and Woodson, H.H., Electromechanical Dynamics Part II: Fields, Forces, and Motion, John Wiley and Sons, Inc., 1968.

34. Abramowitz, M. and Stegun, I.A., Handbook of Mathematical Functions, Dover Publications, Inc., Fifth Printing.